1. 上記単一方程式の左辺は，R_2 が従属変数であることを除いて，線形波動方程式 (38) と同形であるが，すでに，変数 φ を導入したことによって自動的にゼロとなる．
2. 近傍場を記述する方程式系 (33)-(36) を，φ に対する偏導関数のみから構成される偏微分方程式としてまとめ直した後に，φ に関する不定積分を行い，従属変数間を関係付ける代数関係式群を得る．
3. 方程式系 (42)-(46) における，独立変数として φ と t_1 にしたがう非同次項 $f_i\,(i=1,2,3,4,5)$ は，α_1, u_{G1}, u_{L1}, p_{L1}, R_1 の，φ に関する 2 次の偏導関数項，および，t_1 に関する 1 次の偏導関数項の線形結合から形成されるが，この両者ともに，事項 2. の利用によって，単一変数 R_1 の偏導関数項のみで表現し直すことが可能である．

上記の操作を実行することによって，遠方場を記述する，単一の 3 階非線形偏微分方程式を導出することができる：

$$\frac{\partial R_1}{\partial t_1}+C_1R_1\frac{\partial R_1}{\partial\varphi}+C_2\frac{\partial^2R_1}{\partial\varphi^2}+C_3\frac{\partial^3R_1}{\partial\varphi^3}=0. \qquad (47)$$

ここに，C_1, C_2, C_3 は諸定数から形成される係数であるが，その陽的な形は本稿では差し控える．

式 (47) は，気泡流中において，分散性と散逸性ならびに 2 次の非線形性をあわせもつ波動現象を記述する Korteweg-de Vries-Burgers 方程式である．線形波動方程式 (38) および K-dV-Burgers 方程式 (47) は，近傍場においては無視できた分散，散逸，非線形の効果が，遠方場において，同時に発現しうることを示している．諸定数のオーダーの適切な選定 (29) のもとで，3 圧力 2 流体モデルに基づく質量および運動量の保存則 (1)-(4)，および Keller の方程式 (7) という，5 本もの偏微分方程式系の 5 つの従属変数群の 2 次摂動項を考慮することによって，式 (47) の導出に至ることができた．

その導出過程をふりかえればわかるように，分散項は Keller の方程式の 2 階導関数項 (左辺第 1 項) に起因し，散逸項は 1 階導関数 (音響放射減衰) 項 (右辺第 2 項) に起因する．また，非線形項は，4 つの保存則および Keller の方程式のすべてに起因している．なかでも，散逸項が，媒質の粘性や熱伝導性に起因するのではなく，液相圧縮性の効果による，気泡の減衰振動 (音響放射減衰) に起因することは，特筆すべき差異である．液相を非圧縮性とみなして，K-dV-Burgers 方程式の導出を試みた既知研究 [3] においては，その散逸項は，粘性あるいは熱伝導性にしか由来しえないからである．

従来の解析との差異のより精密な比較，また諸係数 C_1, C_2, C_3 の定義など，詳細は講演時に述べる．

4. 今後の展望

第 1 の展望として，K-dV-Burgers 方程式 (47) を数値的に解くことによって，そのふるまいの把握，とくに非線形効果，散逸効果，分散効果の定量的把握をすることが挙げられる．また，音響放射減衰のみならず，流体の粘性および熱伝導性の考慮による散逸効果をも含む K-dV-Burgers 方程式の導出も展望である．

さらに，はじめに述べたように，医療応用を見据えるという目的からは，殻付き気泡の振動特性を踏まえる必要がある．すでに，Hoff らが，非圧縮性液体中における単一の粘弾性殻付き球形気泡の振動を記述する方程式 [1] を導いている：

$$\rho_L^*\left[R^*\frac{\mathrm{d}^2R^*}{\mathrm{d}t^{*2}}+\frac{3}{2}\left(\frac{\mathrm{d}R^*}{\mathrm{d}t^*}\right)^2\right]=P^*$$
$$-12\frac{d_0^*R_0^*}{R^{*3}}\left[G_s^*\left(1-\frac{R_0^*}{R^*}\right)+\frac{\mu_s^*}{R^*}\frac{\mathrm{d}R^*}{\mathrm{d}t^*}\right]. \qquad (48)$$

ここに，d_0^* は初期静止平衡状態における殻の厚さ，また G_s^* と μ_s^* は，それぞれ，殻の振動に起因する剛性率 (横弾性係数) および粘性率である (他記号の定義は本稿中の記述と同一，また諸変数と係数はすべて有次元)．

式 (48) は，液相の粘性および表面張力を無視した Rayleigh-Plesset の式 (左辺，および右辺第 1 項が相当する) と，殻の弾性に起因する項 (右辺第 2 項)，また殻の粘性に起因する項 (右辺第 3 項)，これらの線形結合により形成されている．殻の弾性および粘性の効果を考慮した上での気泡振動の，波のふるまいへ与える影響を，定性的および定量的に知ることが強く望まれる．

本稿では，殻の存在自体を考慮しなかったが，今後，圧縮性を考慮した液体中における殻付き気泡の振動を記述する方程式を，Hoff ら [1] や Keller ら [7] に倣って導出することを試み，支配方程式系に組み込み直すことによって，本理論の医学への応用をも目指す．

謝辞

本研究は，平成 20 度厚生労働省科学研究費補助金 (医療機器開発推進研究事業：ナノメディシン研究 (H19-nano-010) によりなされたものである．ここに記して謝意を表す．

参考文献

(1) Hoff, L., Sontum, P. C. and Hovem, J. M., "Oscillations of polymeric microbubbles: Effect of the Encapsulating Shell," *J. Acoust. Soc. Am.*, **107** (2000), pp. 2272–2280.
(2) van Wijingaarden, L., "On the equation of motion for mixtures of liquid and gas bubbles," *J. Fluid. Mech.*, **33** (1968), pp. 465–474.
(3) van Wijingaarden, L., "One-dimensional flow of liquids containing small gas bubbles," *Annu. Rev. Fluid Mech.*, **4** (1972), pp. 369–396.
(4) Egashira, R., Yano, T. and Fujikawa, S., "Linear wave propagation of fast and slow modes in mixtures of liquid and gas bubbles," *Fluid Dyn. Res.*, **34** (2004), pp. 317–334.
(5) Yano, T., Egashira, R. and Fujikawa, S., "Linear analysis of dispersive waves in bubbly flows based on averaged equations," *J. Phys. Soc. Jpn.*, **75** (2006), pp. 104401-01-08.
(6) Eames, I. and Hunt, J. C. R., "Forces on bodies moving unsteadily in rapidly compressed flows," *J. Fluid Mech.*, **505** (2004), pp. 349–364.
(7) Keller, J. B. and Miskis, M., "Bubble oscillations of large amplitude," *J. Acoust. Soc. Am.*, **68** (1980), pp. 628–633.

Proceedings of CAV2009
Seventh International Symposium on Cavitation
August 17-22, 2009, Ann Arbor, Michigan, USA

WEAKLY NONLINEAR ANALYSIS OF DISPERSIVE WAVES IN MIXTURES OF LIQUID AND GAS BUBBLES BASED ON A TWO-FLUID MODEL

Tetsuya KANAGAWA
Division of Mechanical & Space Engineering
Hokkaido University, Sapporo, Japan
kanagawa@mech-me.eng.hokudai.ac.jp

Takeru YANO
Division of Mechanical Engineering
Osaka University, Suita, Japan
yano@mech.eng.osaka-u.ac.jp

Masao WATANABE
Division of Mechanical & Space Engineering
Hokkaido University, Sapporo, Japan
masao.watanabe@eng.hokudai.ac.jp

Shigeo FUJIKAWA
Division of Mechanical & Space Engineering
Hokkaido University, Sapporo, Japan
fujikawa@eng.hokudai.ac.jp

ABSTRACT

The characteristics of sound waves in bubbly liquids are considerably different from those in single phase fluids [1, 2]. Especially, the dispersion in the sense that waves of different wavelengths propagate with different phase velocities is an important property, which is caused by bubble oscillations.

In the present paper, the one-dimensional nonlinear dispersive waves in the liquid containing a number of small spherical gas bubbles (see Fig. 1) are theoretically studied on the basis of a set of two-fluid averaged equations derived by the present authors [3,4]. The set of equations is composed of the conservation laws of mass and momentum for gas and liquid phases [3], the Keller equation of the oscillations of spherical gas bubble [5], the equations of state for gas and liquid phases, the law of mass conservation of the gas inside each bubble, and the pressure balance at the gas-liquid interface. At an initial state, the mixtures are assumed to be uniform and at rest. The compressibility of liquid phase is taken into account. For the simplicity, we neglect the viscosity, thermal conductivity, phase change across the interface, and Reynolds stress.

Egashira *et al.* [3] analyzed linear pressure waves in the bubbly liquid on the basis of the two-fluid model, and showed the existence of the two modes, i.e., slow mode and fast mode, by considering the compressibility of liquid. Figure 2 shows the linear dispersion relation of slow mode [3]. Band A and Band B in Fig. 2 are correspondent to the moderately low and high frequency bands, respectively. Here, Band A is regarded as the weakly dispersive band. We firstly analyze the weakly nonlinear propagation of pressure waves in Band A by an appropriate scaling of parameters.

Now, let us define the scaling of three parameters, i.e., the characteristics velocity U, the characteristics length L, and the

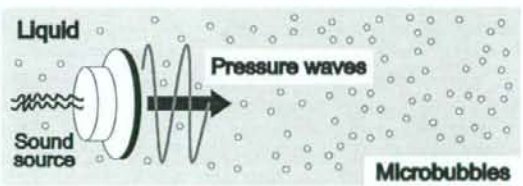

Figure 1. Schematic of the problem. Pressure waves in the liquid containing a number of small spherical gas bubbles generated by oscillations of the sound source. The mixtures are uniform and at rest at an initial state.

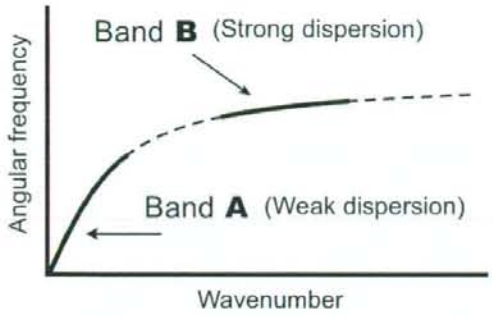

Figure 2. The dispersion relation of the slow mode in a bubbly quiescent liquid [3]. Band A and Band B indicate the weakly and strongly dispersive bands, respectively.

characteristics time T, as follows:

$$T\omega_B\sqrt{\varepsilon} \equiv O(1) \equiv \Omega, \tag{1}$$

$$\frac{U}{c_{L0}\sqrt{\varepsilon}} \equiv O(1) \equiv V, \tag{2}$$

$$\frac{R_0}{L\sqrt{\varepsilon}} \equiv O(1) \equiv \Delta, \tag{3}$$

where $\varepsilon (\ll 1)$ is a nondimensional typical wave amplitude, ω_B is the eigenfrequency of the single bubble of the initial radius R_0, c_{L0} is the speed of sound in the liquid in an unperturbed state, and Ω, V, and Δ are nondimensional constants of $O(1)$. The velocity U is a typical propagation speed of waves, the time $T = 1/\omega$ is its typical period (ω is a frequency of the sound source), and $L = UT$ is its typical wavelength.

All dependent variables are nondimensionalized and then expanded in a power series of ε. Here, we shall remark that only the perturbation expansion of the density of liquid phase begins with $O(\varepsilon^2)$. By substituting the expansions into the system of governing equations and using the scalings (1)-(3), we can derive the equation of the near field characterized by L and T. As a result, the near field is described by the linear wave equation. Therefore, the near field can be regarded as a nondispersive and nondissipative region in the present analysis based on the scalings (1)-(3).

Let us proceed to the derivation of equation in a far field, where the weak dispersion effect and weak dissipation effect appear and compete with the weak nonlinear effect. We shall introduce the two time scales $t_0 = t$ and $t_1 = \varepsilon t$ (t is the nondimensional time). The far field equation, the Korteweg–de Vries–Burgers (KdV-Burgers) equation can be derived by the use of multiple scales, as follows:

$$\frac{\partial f}{\partial t_1} + C_1 f\frac{\partial f}{\partial \varphi} + C_2\frac{\partial^2 f}{\partial \varphi^2} + C_3\frac{\partial^3 f}{\partial \varphi^3} = 0, \tag{4}$$

where $\varphi = x - vt_0$ is the nondimensional phase angle of the right-running wave (x is the nondimensional space coordinate normal to the wavefront, $v = 1 - \varepsilon\Omega^2V^2\Delta^2(1-\alpha_0)/(6\alpha_0)$ is the phase velocity of waves in the far field, and α_0 is the void fraction in the unperturbed state), and $f(t_1, \varphi)$ is the leading order approximation of the nondimensional bubble radius. Here, the coefficients of dissipative and dispersive terms in Eq. (4), C_2 and C_3 are given by

$$C_2 = -\frac{\Omega^2V\Delta^3}{6\alpha_0}, \quad C_3 = \frac{\Delta^2}{6\alpha_0}. \tag{5}$$

The explicit representation of the coefficient C_1 will be shown in the final technical paper because of the complexity of expression.

The KdV-Burgers equation (4) describes the weakly nonlinear propagation of waves with dissipative and dispersive effects. The third term in Eq. (4) is derived from the effect of the attenuation of bubble oscillations due to acoustic radiation, i.e., the consideration of the compressibility of liquid phase.

Furthermore, the propagation of linear pressure waves in the moderately high frequency band (see Band B in Fig. 2), which have strongly dispersive effects, is analyzed by the present authors [6]. We extend the problem to the weakly nonlinear problem. The result will be shown in the final technical paper.

ACKNOWLEDGEMENTS

This work was carried out by the aid of Research on Advanced Medical Technology, Ministry of Health, Labor and Welfare (H19-nano-010). The authors would like to express their deepest gratitude towards this grant.

REFERENCES

[1] van Wijingaarden, L., 1968, *J. Fluid Mech.*, **33**, 465-474.
[2] van Wijingaarden, L., 1972, *Annu. Rev. Fluid Mech.*, **4**, 369-396.
[3] Egashira, R., Yano, T. and Fujikawa, S., 2004, *Fluid Dyn. Res.*, **34**, 317-334.
[4] Yano, T., Egashira, R. and Fujikawa, S., 2006, *J. Phys. Soc. Jpn.*, **75**, 104401-01-08.
[5] Keller, J. B. and Kolodner, I. I., 1956, *J. Appl. Phys.*, **27**, 1152-1161.
[6] Haga, T., Yano, T. and Fujikawa, S., 2008, *Proc. 7th JSME-KSME Thermal and Fluids Engineering Conference*, Japan.

キャビテーションに関するシンポジウム (第 14 回)
2009.3.19–20· 仙台市

2 流体モデルに基づく 気泡含有液体中を伝播する分散性波動に対する弱非線形解析

Weakly Nonlinear Analysis of Dispersive Waves in Bubbly Liquid Based on Two-Fluid Model

○ 金川 哲也 (北大)　矢野　猛 (阪大)　渡部 正夫 (北大)　藤川 重雄 (北大)

Tetsuya Kanagawa, Graduate School of Engineering, Hokkaido University, Sapporo, 060-8628
Takeru Yano, Graduate School of Engineering, Osaka University, Suita, 565-0871
Masao Watanabe, Graduate School of Engineering, Hokkaido University, Sapporo, 060-8628
Shigeo Fujikawa, Graduate School of Engineering, Hokkaido University, Sapporo, 060-8628

One-dimensional nonlinear dispersive waves in a bubbly liquid is studied theoretically based on a two-fluid model composed of the conservation laws of mass and momentum for gas and liquid phases, and the Keller equation for the dynamics of the spherical bubble. The compressibility of the liquid phase is taken into account, and this leads to the wave attenuation due to bubble oscillations. We focus on the moderately high frequency band regarded as the strongly dispersive band. By using the method of multiple scales, we can derive the nonlinear Schrödinger equation with an attenuation term due to acoustic radiation from bubbles. This equation describes a far field of nearly monochromatic wave train in bubbly liquids, which evolves into a slowly modulated wave packet as a result of long range propagation of weakly nonlinear waves with strong dispersion effect.

Keywords: Weakly nonlinear wave, Bubbly liquid, Strong dispersion, Acoustic radiation, Nonlinear Schrödinger equation

1 はじめに

Egashira らによって, キャビテーションによって生じる気泡近傍の局所的高圧や, 気泡を含む圧縮性液体中に放射される強い圧力波を記述できる, 2 流体モデルに基づく 気泡流の方程式系が導出された [1]. われわれは, この方程式を起点とした, 線形波動伝播の解析を行ってきた [1, 2].

また, 非線形効果を取り 入れた解析として, 球形微細気泡を多数含む圧縮性液体中における, 波長の長い圧力変動が, 気泡の固有振動数に比べて小さな周波数のもとで伝播するとき, 十分な距離を伝播した後におけるふるまいが K-dV-Burgers 方程式で記述されることを示した [3]. さらに, 気泡の固有振動数と 圧力変動の周波数が同程度, および, 波長が短い圧力波に対する線形伝播過程を調べた [4]. これらの両解析において, 分散性の効果が, 前者の問題設定 [3] では波長に比べ十分な距離を伝播するまではあらわれないのに対し, 後者の設定 [4] においては数波長程度の距離を伝播する間にあらわれる. 比較するならば, 後者は, 前者より 強い分散性を示す周波数帯に注目しているといえる.

一般に, ある種の強分散性媒質中において, 特定の波数および周波数のまわり に狭い広がり を持つ準単色波列を考える. このとき, 弱い非線形効果も 考慮すると, 搬送波はゆるやかな変化を受け, 搬送波の包絡線の振幅の時間発展は, 非線形 Schrödinger 方程式によって記述される [5]. 非線形 Schrödinger 方程式の 1 つの定常進行波解として, 図 1 に, 包絡ソリトン (または, ブライトソリトン) の波形を示す.

本報告では, 先の報告 [4] を, 非線形問題へ拡張し, 多数の微細気泡を含む圧縮性液体中における高周波数および短波長の, 準単色波列の非線形効果による 変調を取り 扱う. その過程は, 非線形 Schrödinger 方程式に, 液相の圧縮性に由来する音響放射減衰に伴う 項を付加した式で記述されることが示される.

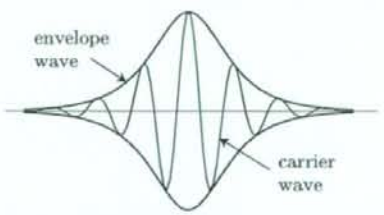

Fig. 1: Waveform of the envelope soliton as a solution of the nonlinear Schrödinger equation.

2 問題設定および基礎方程式

多数の微細な球形気泡を含む液体中に音源が設置されており, その位置を原点 O とする 1 次元空間座標 x^* を設定する. 音源から, 角振動数 ω^* のもとで, x^* 軸の正方向へ, 平面波が放射されている状況を考える. なお, $*$ を, すべての有次元変数および有次元定数に付けて, 無次元量と 区別する.

2.1 基礎方程式系　気泡流の運動は, Egashira らによって提案された, 2 流体モデルに基づく 気相と 液相それぞれに対する質量および運動量の保存則 [1] で記述される:

$$\frac{\partial}{\partial t^*}(\alpha\rho_G^*) + \frac{\partial}{\partial x^*}(\alpha\rho_G^* u_G^*) = 0, \tag{1}$$

$$\frac{\partial}{\partial t^*}[(1-\alpha)\rho_L^*] + \frac{\partial}{\partial x^*}[(1-\alpha)\rho_L^* u_L^*] = 0, \tag{2}$$

$$\frac{\partial}{\partial t^*}(\alpha\rho_G^* u_G^*) + \frac{\partial}{\partial x^*}\left(\alpha\rho_G^* {u_G^*}^2\right) + \alpha\frac{\partial p_G^*}{\partial x^*} = F^*, \tag{3}$$

$$\frac{\partial}{\partial t^*}\left[(1-\alpha)\rho_L^* u_L^*\right] + \frac{\partial}{\partial x^*}\left[(1-\alpha)\rho_L^* {u_L^*}^2\right] + (1-\alpha)\frac{\partial p_L^*}{\partial x^*} + P^*\frac{\partial \alpha}{\partial x^*} = -F^*, \tag{4}$$

ここに, t^* は時間, x^* は 1 次元空間座標 (波面に垂直), α は気相の体積率 (ボイド率), u^* は流速, ρ^* は流体の密度, p^* は圧力, P^* は気液界面における局所的な液相圧力, F^* は単位時間・単位体積あたりの気液の相間の運動量輸送を表し, また下添え字 G と L は, それぞれ, 気相に属する変数と液相に属する変数を意味する.

運動量保存則 (3)(4) の右辺における相間の運動量輸送項 F^* には, 液相の圧縮性を考慮できるように拡張された付加慣性力 [6] を考慮したモデル [2]

$$F^* = -\beta_1\alpha\rho_L^*\left(\frac{\mathrm{D}_G u_G^*}{\mathrm{D}t^*} - \frac{\mathrm{D}_L u_L^*}{\mathrm{D}t^*}\right) - \beta_2\rho_L^*(u_G^* - u_L^*)\frac{\mathrm{D}_G\alpha}{\mathrm{D}t^*} - \beta_3\alpha(u_G^* - u_L^*)\frac{\mathrm{D}_G\rho_L^*}{\mathrm{D}t^*}, \quad (5)$$

を採用する. ここに, 係数 β_i $(i = 1,2,3)$ はふつう 3 つとも 1/2 とすればよく, また, $\mathrm{D}_G/\mathrm{D}t^*$ と $\mathrm{D}_L/\mathrm{D}t^*$ は, それぞれ, 以下のように定義される:

$$\frac{\mathrm{D}_G}{\mathrm{D}t^*} \equiv \frac{\partial}{\partial t^*} + u_G^*\frac{\partial}{\partial x^*}, \quad \frac{\mathrm{D}_L}{\mathrm{D}t^*} \equiv \frac{\partial}{\partial t^*} + u_L^*\frac{\partial}{\partial x^*}. \quad (6)$$

気泡壁の運動方程式として, 圧縮性液体中における気泡の膨張・収縮運動を記述できる, Keller の方程式 [7]

$$\left(1 - \frac{1}{c_{L0}^*}\frac{\mathrm{D}_G R^*}{\mathrm{D}t^*}\right)R^*\frac{\mathrm{D}_G^2 R^*}{\mathrm{D}t^{*2}} + \frac{3}{2}\left(1 - \frac{1}{3c_{L0}^*}\frac{\mathrm{D}_G R^*}{\mathrm{D}t^*}\right)\left(\frac{\mathrm{D}_G R^*}{\mathrm{D}t^*}\right)^2 = \left(1 + \frac{1}{c_{L0}^*}\frac{\mathrm{D}_G R^*}{\mathrm{D}t^*}\right)\frac{P^*}{\rho_{L0}^*} + \frac{R^*}{\rho_{L0}^* c_{L0}^*}\frac{\mathrm{D}_G}{\mathrm{D}t^*}(p_L^* + P^*), \quad (7)$$

を用いる. ここに, R^* は気泡径であり, c_{L0}^* および ρ_{L0}^* は, それぞれ, 初期静止状態における液相の音速および密度である. 式 (7) の右辺第 2 項が, 音響放射減衰の効果を表す.

その他の従属変数として, p_G^*, p_L^*, P^*, ρ_G^* は, 以下に示す, 気相に対するポリトロープ変化の関係式, 液相に対する状態方程式 (Tait の式を変形したもの), 気液界面における圧力のつり合い式, 気泡内気体の質量保存則から計算される:

$$p_G^* = \left(\frac{\rho_G^*}{\rho_{G0}^*}\right)^\gamma p_{G0}^*, \quad (8)$$

$$p_L^* = p_{L0}^* + \frac{\rho_{L0}^* c_{L0}^{*2}}{n}\left[\left(\frac{\rho_L^*}{\rho_{L0}^*}\right)^n - 1\right], \quad (9)$$

$$P^* = p_G^* - p_L^* - \frac{2\sigma^*}{R^*}, \quad (10)$$

$$\rho_G^* = \left(\frac{R_0^*}{R^*}\right)^3 \rho_{G0}^*, \quad (11)$$

ここに, ρ_{G0}^*, p_{G0}^*, p_{L0}^* は, それぞれ, 初期状態における気相密度, 気相圧力, 液相圧力, σ^* は表面張力, γ はポリトロープ指数, n は物質定数である.

初期に, 媒質は静止状態にあり, また気泡径を含むすべての物理量が一様であるとする. さらに, 媒質の粘性, 熱伝導性, また気液界面を通しての相変化および物質輸送を無視する.

2.2 高周波数, 短波長の弱非線形波動 以下に示す 5 つの従属変数について, 波の代表的な無次元振幅 ϵ $(\ll 1)$ を用いて, 摂動展開する:

$$\alpha/\alpha_0 = 1 + \epsilon\alpha_1 + \epsilon^2\alpha_0 + \cdots, \quad (12)$$

$$u_G^*/U^* = \epsilon u_{G1} + \epsilon^2 u_{G2} + \cdots, \quad (13)$$

$$u_L^*/U^* = \epsilon u_{L1} + \epsilon^2 u_{L2} + \cdots, \quad (14)$$

$$R^*/R_0^* = 1 + \epsilon R_1 + \epsilon^2 R_2 + \cdots, \quad (15)$$

$$\rho_L^*/\rho_{L0}^* = 1 + \epsilon^3\rho_{L1} + \epsilon^4\rho_{L2} + \cdots, \quad (16)$$

ここに, α_0 と R_0^* は, それぞれ, 初期状態におけるボイド率と気泡径, U^* は波の代表的な速さである. また, 無次元液相密度 ρ_L^*/ρ_{L0}^* の展開を, $O(\epsilon^3)$ から始めることを注意しておく.

場を特徴づける, 代表的なスケールとしての速度 U^*, 長さ L^*, 時間 T^* に対して, それぞれ

$$\frac{\omega^*}{\omega_B^*} \equiv O(1) \equiv \quad , \quad (17)$$

$$\frac{R_0^*}{L^*} \equiv O(1) \equiv \quad , \quad (18)$$

$$\frac{U^*}{\epsilon\, c_{L0}^*} \equiv O(1) \equiv V, \quad (19)$$

と定める. ここに, 波の代表的なスケールとして, T^* は周期, L^* は波長, $U^* = L^*/T^*$ は伝播速度を表す. また, , , V はすべて $O(1)$ の定数であり, ω_B^* は半径 R_0^* の単一気泡の固有角振動数 (減衰なし) である:

$$\omega_B^* \equiv \sqrt{\frac{3\gamma p_{G0}^* - 2\sigma^*/R_0^*}{\rho_{L0}^* R_0^{*2}}}. \quad (20)$$

オーダー評価 (17)-(19) は, それぞれ, 波の周波数が気泡の固有振動数と同程度であること, 波の波長が気泡径と同程度であること, 波の伝播速度の液単相音速に対する比率が $O(\sqrt{\epsilon})$ 程度の大きさであることを意味する. ここで, 平均化方程式 (1)-(4) は, ふつうは, (18) で定められるような短波は記述できないが, 平面波問題においては, 波面に平行な方向に, 多数の気泡が含まれるような十分に大きい平均化体積を設置可能であることから, 本問題に適用可能といえる [4].

液相圧力 p_L^* は, 式 (16), (9) および (19) を用いて

$$p_L^* = p_{L0}^* + \epsilon\rho_{L0}^* U^{*2} p_{L1} + \epsilon^2\rho_{L0}^* U^{*2} p_{L2} + \cdots, \quad (21)$$

と展開される. ここに, 無次元液相圧力 p_{Li} $(i = 1,2,3)$ は, 定数 V を用いて, 無次元液相密度と結びつけて

$$p_{L1} = \frac{\rho_{L1}}{V^2}, \quad p_{L2} = \frac{\rho_{L2}}{V^2}, \quad p_{L3} = \frac{\rho_{L3}}{V^2}, \quad (22)$$

と導入している. なお, 本稿では p_{L3} までしか現れないが, p_{L4} は ρ_{Li} $(i = 1,2,3,4)$ を用いて表されることを注意しておく (さらに高次のものも同様).

波の代表的な周期 T^* を, 気泡の固有角振動数 ω_B^* の逆数を用いて定める:

$$T^* \equiv \frac{1}{\omega_B^*}. \quad (23)$$

また, 初期静止状態における気相圧力 p_{G0}^* を

$$\hat{p}_{G0} \equiv \frac{p_{G0}^*}{\rho_{L0}^* U^{*2}} \equiv O(1), \quad (24)$$

のように無次元化およびオーダー評価し ($\hat{p}_{G0}$ は無次元の初期気相圧力), さらに, 初期液相密度に対する初期気相密度の比が, $O(\epsilon^3)$ 程度の小ささであると仮定する:

$$\frac{\rho_{G0}^*}{\rho_{L0}^*} \equiv O(\epsilon^3). \quad (25)$$

3 特異摂動法による解析

3.1 多重尺度法 [8] 時間 t^*, および, 空間座標 x^* を

$$t^* = T^* t, \quad x^* = L^* x, \tag{26}$$

と無次元化し, 無次元振幅 ϵ を用いて, 無次元時間 t と無次元空間座標 x に対する, slow variables を定義する:

$$\begin{aligned} &t_0 = t, \quad t_1 = \epsilon t, \quad t_2 = \epsilon^2 t, \ldots \\ &x_0 = x, \quad x_1 = \epsilon x, \quad x_2 = \epsilon^2 x, \ldots \end{aligned} \tag{27}$$

ある従属変数 $f(t_0, t_1, t_2, x_0, x_1, x_2, \ldots)$ に対して, t と x に対する偏導関数は, slow variables を用いて, 以下のように展開される:

$$\begin{aligned} \frac{\partial f}{\partial t} &= \frac{\partial f}{\partial t_0} + \epsilon \frac{\partial f}{\partial t_1} + \epsilon^2 \frac{\partial f}{\partial t_2} + \cdots, \\ \frac{\partial f}{\partial x} &= \frac{\partial f}{\partial x_0} + \epsilon \frac{\partial f}{\partial x_1} + \epsilon^2 \frac{\partial f}{\partial x_2} + \cdots. \end{aligned} \tag{28}$$

3.2 線形方程式系 従属変数の摂動展開, パラメータのオーダー評価, また slow variables の定義などを, 基礎方程式系に代入し, ϵ の恒等式として整理してゆく.

まず, $O(\epsilon)$ の方程式系として, 以下を得る (順に, 気相および液相の質量保存則と運動量保存則, Keller の方程式を表す):

$$\frac{\partial \alpha_1}{\partial t_0} - 3\frac{\partial R_1}{\partial t_0} + \frac{\partial u_{G1}}{\partial x_0} = 0, \tag{29}$$

$$-\alpha_0 \frac{\partial \alpha_1}{\partial t_0} + (1-\alpha_0)\frac{\partial u_{L1}}{\partial x_0} = 0, \tag{30}$$

$$\beta_1 \frac{\partial u_{G1}}{\partial t_0} - \beta_1 \frac{\partial u_{L1}}{\partial t_0} - 3\gamma \tilde{p}_{G0} \frac{\partial R_1}{\partial x_0} = 0, \tag{31}$$

$$\begin{aligned} &-\alpha_0\beta_1 \frac{\partial u_{G1}}{\partial t_0} + (1-\alpha_0+\beta_1\alpha_0)\frac{\partial u_{L1}}{\partial t_0} \\ &\qquad + (1-\alpha_0)\frac{\partial p_{L1}}{\partial x_0} = 0, \end{aligned} \tag{32}$$

$$\frac{\partial^2 R_1}{\partial t_0^2} + R_1 + \frac{p_{L1}}{{}^2} = 0. \tag{33}$$

方程式系 (29)-(33) は, R_1 を従属変数とする, 単一線形偏微分方程式

$$\begin{aligned} \mathcal{L}_1[R_1] \equiv &\frac{\partial^2 R_1}{\partial t_0^2} - \frac{{}^2}{3\alpha_0}\frac{\partial^4 R_1}{\partial x_0^2 \partial t_0^2} \\ &- \left[\frac{{}^2}{3\alpha_0} + \frac{(1-\alpha_0+\beta_1)\gamma\tilde{p}_{G0}}{\beta_1(1-\alpha_0)}\right]\frac{\partial^2 R_1}{\partial x_0^2} = 0, \end{aligned} \tag{34}$$

にまとめられる. なお, 以後の表記のため, 線形演算子 $\mathcal{L}_1$ を導入した.

式 (34) の解を, 以下のように仮定する:

$$R_1 = A e^{i\theta} + c.c., \tag{35}$$

ここに, $A(t_1, x_1, t_2, x_2, \ldots)$ は slow variables に依存して時間および空間的にゆっくり変化する複素振幅である. なお, 記号 c.c. はその記号より左側にあるすべての複素数の複素共役を表し, i は虚数単位である. また, θ は位相関数であり

$$\theta \equiv k^* x_0^* - \omega^* t_0^* = k x_0 - \quad t_0, \tag{36}$$

と表される (無次元波数 $k = k^* L^*$ を導入).

解 (35) を, 方程式系 (29)-(33) に代入し, t_0 や x_0 で積分して初期条件や無限遠方の境界条件を考慮すれば, 1 次の摂動項 $\alpha_1, u_{G1}, u_{L1}, p_{L1}$ を順次得る. それらはすべて, R_1 の定数倍で表される.

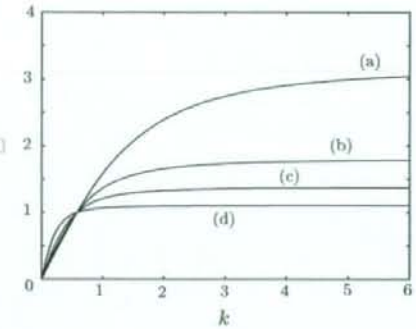

Fig. 2: Linear dispersion relation in the case of $\gamma = 1$, $\beta_1 = 1/2$ and $\tilde{p}_{G0} = 1$: (a) $\alpha_0 = 10^{-2}$, $\quad = 0.1$, (b) $\alpha_0 = 10^{-2}$, $\quad = 0.2$, (c) $\alpha_0 = 10^{-3}$, $\quad = 0.1$ and (d) $\alpha_0 = 10^{-3}$, $\quad = 0.1$.

3.3 線形分散関係式と位相速度, 群速度 式 (34) に解 (35) を代入すれば, 線形分散関係式

$$\begin{aligned} D(k, \quad) = &\frac{{}^2 k^2 (1 - \quad ^2)}{3\alpha_0} \\ &+ \frac{(1-\alpha_0+\beta_1)\gamma\tilde{p}_{G0}}{\beta_1(1-\alpha_0)}k^2 - \quad ^2 = 0, \end{aligned} \tag{37}$$

を得る. ここで, $\quad$ と α_0 を適当に選び 4 通りの場合についての分散関係を, 図 2 に示す.

無次元位相速度 v_p, 無次元群速度 v_g を, それぞれ

$$v_p \equiv \frac{v_p^*}{U^*}, \quad v_g \equiv \frac{v_g^*}{U^*}, \tag{38}$$

と定義する. ここに, $v_p^* = \omega^*/k^*$ は位相速度, $v_g^* = \mathrm{d}\omega^*/\mathrm{d}k^*$ は群速度である. 無次元位相速度, 無次元群速度, また群速度の波数での 1 階微分は, それぞれ, 以下のように与えられる:

$$v_p = \frac{}{k}, \tag{39}$$

$$v_g = \frac{3\alpha_0}{k(3\alpha_0 + \quad ^2 k^2)}, \tag{40}$$

$$\frac{\mathrm{d}v_g}{\mathrm{d}k} = -\frac{9\alpha_0 \quad ^2}{(3\alpha_0 + \quad ^2 k^2)^2}. \tag{41}$$

3.4 代表スケールの決定 代表的な周期の決定 (23) に続いて, 代表的な速度 U^* および長さ L^* を決定する. $\omega^* \equiv \omega_B^*$ (すなわち $\quad \equiv 1$) と定めた上で, $v_g = 1$ を満足するような U^* と L^* を選ぶ. すなわち

$$L^* \equiv \frac{3\alpha_0}{k^*(3\alpha_0 + R_0^{*2} k^{*2})}, \quad U^* \equiv \frac{3\alpha_0 \omega_B^*}{k^*(3\alpha_0 + R_0^{*2} k^{*2})}, \tag{42}$$

と定める. さらに, 群速度 v_g を 1 と定めたことから

$$\frac{3\alpha_0}{k(3\alpha_0 + \quad ^2 k^2)} = 1, \tag{43}$$

の関係を得る. 同時に, 式 (18) および (19) も満足する必要がある.

3.5　2次の解析より得る遠方場の方程式　つづいて，$O(\epsilon^2)$ の方程式系を導出したのちに，3.2 節とおなじく，R_2 を未知変数とする単一式にまとめる：

$$\mathcal{L}[R_2] = -\frac{1}{3}\frac{\partial N_1}{\partial t_0} - \frac{1}{3\alpha_0}\frac{\partial N_2}{\partial t_0} + \frac{1-\alpha_0+\beta_1}{3\beta_1(1-\alpha_0)}\frac{\partial N_3}{\partial x_0} + \frac{1}{3\alpha_0(1-\alpha_0)}\frac{\partial N_4}{\partial x_0} - \frac{^2}{3\alpha_0}\frac{\partial^2 N_5}{\partial x_0^2} \equiv H_2. \quad (44)$$

式 (44) の非同次項 H_2 は，R_1 や u_{G1} などの 1 次の摂動項から形成される．それらを代入し，整理すれば

$$H_2 = \hat{C}A^2 e^{2i\theta} + i\left(-\frac{\partial D}{\partial}\right)\left(\frac{\partial A}{\partial t_1} + v_g\frac{\partial A}{\partial x_1} + CA\right)e^{i\theta} + c.c., \quad (45)$$

を得る (係数 $\hat{C}$ の陽な表現は複雑ゆえ省略)．

H_2 には，$e^{i\theta}$ および $e^{-i\theta}$ に比例する項が含まれており，このままでは永年項が生じて漸近展開 (12)-(16) が一様に有効とはならない．よって，永年項が現れないための条件 (可解条件)

$$\frac{\partial A}{\partial t_1} + v_g\frac{\partial A}{\partial x_1} + CA = 0, \quad C = \frac{V\ ^3k^2}{2(3\alpha_0 + \ ^2k^2)}, \quad (46)$$

を課す．以後，式 (46) を，t_1 に関する導関数と，x_1 に関する導関数を変換する際に使用する．偏微分方程式 (46) の一般解，すなわち，複素振幅 A の t_1 と x_1 に関する遠方場におけるふるまいは

$$A(t_1, x_1) = B(\varphi)\exp(-Ct_1), \quad (47)$$

にしたがう．ここに，B は移動座標 $\varphi = x_1 - v_g t_1$ のみに依存する任意関数である．

R_2 に関する偏微分方程式 (44) の解 (特解) は

$$R_2 = \frac{\hat{C}}{D(2k, 2\ )}A^2 e^{2i\theta} + c.c., \quad (48)$$

で与えられる．なお，式 (44) の同次方程式の一般解は省略した．

つづいて，解 (48) を，$O(\epsilon^2)$ の方程式系に代入することで，u_{G2}, u_{L2}, p_{L2}, α_2 も導くことができる．

3.6　散逸効果を含む非線形 Schrödinger 方程式　$O(\epsilon^3)$ の方程式系を導出し，同様な操作を行う．すなわち，まず，$O(\epsilon^3)$ の 5 つの方程式から，α_3, u_{G3}, u_{L3}, p_{L3} を消去して，R_3 と $O(\epsilon^2)$ までの解析ですでに得られている低次の変数からなる単一の方程式を導出し，これを

$$\mathcal{L}[R_3] = H_3, \quad (49)$$

の形に表す．次に，式 (49) の可解条件にしたがって，非同次項 H_3 の中に含まれる $e^{i\theta}$ に比例する項の係数をゼロとする．

その結果，複素振幅 A の t_2 と x_2 に関する遠方場を記述する，2 階非線形偏微分方程式

$$i\frac{\partial A}{\partial \tau} + \frac{1}{2}\frac{\mathrm{d}^2}{\mathrm{d}k^2}\frac{\partial^2 A}{\partial \xi^2} + \nu_1|A|^2 A + \nu_2 A = 0, \quad (50)$$

を得る．ここで，非線形効果による補正を含む群速度で進む座標系への変数変換として

$$\tau = t_2, \quad \xi = x_1 - (v_g - i\epsilon\nu_3)t_1, \quad (51)$$

とおいた．係数 ν_2 および ν_3 は，音響放射減衰の効果に基づくものである．なお，係数 $\nu_i\,(i = 1, 2, 3)$ の具体的な形は，本稿では省略する．

式 (50) が記述する，包絡波の波形などの，詳細は講演時に述べる．

4　おわりに

2 流体モデルに基づく，気泡を含む圧縮性液体の運動を記述する方程式を起点として，$O(\epsilon^3)$ までの方程式に対する解析から，式 (50) を得た．これは，一般に強分散性媒質中における非線形波動の遠方場を記述する，非線形 Schrödinger 方程式に，音響放射減衰に起因する，複素振幅の定数倍を付加したものとなっている．

今後，その解構造を把握してゆくこと，また弱分散性媒質に対する解析 [3] との比較を行うこと [9] が展望である．

謝辞

本研究は，平成 20 年度厚生労働省科学研究費補助金 (医療機器開発推進研究事業: ナノメディシン研究 (H19-nano-010) によりなされたものである．ここに記して謝意を表す．

参考文献

[1] Egashira, R., Yano, T. and Fujikawa, S., "Linear wave propagation of fast and slow modes in mixtures of liquid and gas bubbles," *Fluid Dyn. Res.*, **34**, 317–334 (2004).

[2] Yano, T., Egashira, R. and Fujikawa, S., "Linear analysis of dispersive waves in bubbly flows based on averaged equations," *J. Phys. Soc. Jpn.*, **75**, 104401–01–08 (2006).

[3] 金川哲也, 矢野 猛, 渡部正夫, 藤川重雄, "殻付き微細気泡群を含む液体中における非線形波の伝播," 日本流体力学会年会 2008 (2008).

[4] Haga, T., Yano, T. and Fujikawa, S., "Propagation characteristics of linear pressure waves in water containing microbubbles," *Proc. 7th JSME-KSME Thermal and Fluids Engineering Conference*, Japan (2008).

[5] Whitham, G. B., *Linear and Nonlinear Waves*, (Wiley, New York, 1974).

[6] Eames, I. and Hunt, J. C. R., "Forces on bodies moving unsteadily in rapidly compressed flows," *J. Fluid Mech.*, **505**, 349–364 (2004).

[7] Keller, J. B. and Kolodner, I. I. "Damping of underwater explosion bubble oscillations," *J. Appl. Phys.*, **27**, 1152–1161 (1956).

[8] Jeffrey, A. and Kawahara, T., *Asymptotic Methods in Nonlinear Wave Theory*, (Pitman Advanced Pub. Program, Boston, 1982).

[9] Kanagawa, T., Yano, T., Watanabe, M. and Fujikawa, S., "Weakly nonlinear analysis of dispersive waves in mixtures of liquid and gas bubbles based on a two-fluid model," *Proc. 7th International Symposium on Cavitation*, America (2009) submitted.

Available online at www.sciencedirect.com
ScienceDirect
Biochemical and Biophysical Research Communications 367 (2008) 590–596
BBRC
www.elsevier.com/locate/ybbrc

Prostaglandin $F_{2\alpha}$ regulates cytokine responses of mast cells through the receptors for prostaglandin E

Izumi Kaneko [a], Takanori Hishinuma [b], Kaori Suzuki [b], Yuji Owada [c], Noriko Kitanaka [c], Hisatake Kondo [c], Junichi Goto [d], Hiroshi Furukawa [a], Masao Ono [a,*]

[a] Department of Pathology, Tohoku University Graduate School of Medicine, 2-1 Seiryo, Aoba-ku, Sendai, Miyagi 980-8575, Japan
[b] Division of Pharmacotherapy, Graduate School of Pharmaceutical Sciences, Tohoku University, Sendai, Japan
[c] Department of Histology, Tohoku University Graduate School of Medicine, Sendai, Japan
[d] Division of Clinical Pharmacology, Tohoku University Hospital, Sendai, Japan

Received 28 December 2007
Available online 9 January 2008

Abstract

There is an increasing body of evidence that prostanoids modulate mast cell functions and contribute to the development of allergic inflammation. The present study aimed to identify an undetermined function of prostaglandin (PG) $F_{2\alpha}$ in mast cell activation and the signaling mechanism involved in it. Simultaneous quantification of prostanoids by liquid chromatography/tandem mass spectrometry revealed the constitutive release of $PGF_{2\alpha}$, thromboxane B_2, and 6-keto-$PGF_{1\alpha}$ from bone marrow-derived mast cells (BMMCs). Upon activation of BMMCs by lipopolysaccharide, the cytokine production in BMMCs was enhanced when the culture was supplemented with $PGF_{2\alpha}$. However, F prostanoid receptor—a selective receptor for $PGF_{2\alpha}$—was not detected in BMMCs. Further investigations performed using prostanoid receptor antagonists revealed an alternative mechanism wherein the receptors for PGE species—E prostanoid receptors—mediated the $PGF_{2\alpha}$ signal in BMMCs. The present study provides an insight into a novel function of $PGF_{2\alpha}$, i.e., an autocrine accelerator for mast cell activation.

Keywords: Mast cell; Lipid mediator; $PGF_{2\alpha}$; Lipopolysaccharide; E prostanoid receptor; EP; Autocrine

Mast cells play a role in the immune and inflammatory responses by sensing a variety of pathogenic patterns through cell-surface receptors. The recruitment of a high-affinity Fc receptor for IgE (FcεRI) by IgE and antigen (hereafter denoted as IgE/Ag) initiates the release of a variety of inflammatory mediators, including histamines, lipid metabolites, and cytokines, occasionally entailing the onset of immediate hypersensitivity and allergic inflammation. On the other hand, mast cells also recognize pathogens in an innate immune mode through other receptors, thus contributing to host defense against bacterial and viral infections. This recognition is mainly achieved by a member of the toll-like receptor (TLR) family, and it subsequently triggers the release of proinflammatory cytokines, including interferons, interleukins, and tumor necrosis factor (TNF)-α, which act in the elimination of pathogens by activating and mobilizing inflammatory cells toward infected sites. Recent studies have shown that a bacterial component, namely, lipopolysaccharide (LPS), enhances FcεRI-mediated mast cell activation [1,2]. Indeed, the co-occurrence of infectious events and the exacerbation of allergic manifestation has been demonstrated in allergic human populations [3–5]. Current findings implicate the contribution of TLR-mediated mast cell activation to the hypersensitivity in allergic diseases in humans.

Membrane lipid metabolites such as prostaglandins (PGs) and leukotrienes (LTs) have been characterized as early mediators that influence the onset of allergic inflammation in mouse models [6–8]. A recent study showed that when the culture of bone marrow-derived mast cells

* Corresponding author. Fax: +81 22 717 8503.
E-mail address: onomasao@mail.tains.tohoku.ac.jp (M. Ono).

0006-291X/$ - see front matter © 2008 Elsevier Inc. All rights reserved.
doi:10.1016/j.bbrc.2008.01.002

(BMMCs) was supplemented with PGE_2 interleukin (IL)-6 production was remarkably enhanced following IgE/Ag simulation [9]. Another study using antagonists specific to an E prostanoid receptor (EP) has shown that EP3 mediates a signal that enhances mast cell activation when supplemented with PGE_2, while EP2 mediates a suppressive signal under the same condition [10]. A study performed using BMMCs derived from EP-deficient strains of mice has proven that EP3 is essential for IL-6 production and degranulation of BMMCs [11]. These findings indicate the contribution of EP2 and EP3 in the regulation of mast cell activation. However, there is little evidence for their role in the production of PGE_1 or PGE_2 in mast cell activation. Paracrine PGE species are considered to be involved in the EP-mediated effects on *in vivo* mast cell activation.

In the present study, we investigated the mechanism of prostanoid-mediated mast cell activation following LPS stimulation using BMMCs. Highly sensitive and simultaneous quantification of prostanoids performed using liquid chromatography/tandem mass spectrometry (LC/MS-MS) revealed constitutive release of $PGF_{2\alpha}$, thromboxane (TX) B_2, and 6-keto-$PGF_{1\alpha}$ into the cultured medium. Functional analyses performed using $PGF_{2\alpha}$ and EP antagonists revealed an enhancing effect of $PGF_{2\alpha}$ on mast cell activation through its heterologous binding to EPs. The present findings provide a novel insight into the role of $PGF_{2\alpha}$ in the regulation of allergenic mast cell response.

Materials and methods

Preparation and activation of BMMC. BMMCs were obtained by culturing mouse bone marrow cells in the RPMI 1640 supplemented with 10% FCS, 1 mM sodium pyruvate, non-essential amino acids, 50 μM 2-mercaptoethanol (SIGMA, St. Louis, MO), and 5 ng/ml murine IL-3 (R&D Systems, Minneapolis, MN). BMMCs were activated with 1 μg/ml trinitrophenyl (TNP) hapten-specific IgE (TNP-IgE) and 1 ng/ml of TNP-conjugated ovalbumin (TNP-OVA) (fraction VII, SIGMA). LPS (*Escherichia coli* 055:B5, SIGMA) was used for the stimulation at 0.1 μg/ml. A cyclooxygenase (Cox) inhibitor, 5-lipooxygenase (Lox) inhibitor, or EP antagonist was incubated for 30 min prior to the supplementation of PG. $PGF_{2\alpha}$, PGE_2, PGD_2 (Cayman chemical, Ann Arbor, MI), and FP agonist Fluprostenol (BIOMOL, Plymouth Meeting, PA) were dissolved in ethanol and were added to the BMMC culture, then incubated for 20 min prior to the stimulation. EP antagonists—ONO-8711 (EP1 antagonist), ONO-AE3-240 (EP3 antagonist), and ONO-AE3-208 (EP4 antagonist)—were kindly donated from Ono pharmaceutics Co. Ltd., Osaka, Japan. Indomethacin (WAKO Pure Chemical, Osaka, Japan), NS-398, SC-560, and NDGA (Cayman chemical) were dissolved in DMSO or ethanol and were added to the BMMC culture with a constant solvent concentration (0.1% DMSO or ethanol). All experiments were performed under non-toxic conditions for any inhibitor dose, which were assessed by cell viability test (data not shown).

Measurements of cytokines and degranulation of BMMC. The concentration of IL-6 and TNF-α in the cultured medium were measured at 6 h after stimulation by enzyme-linked immunosorbent assay (ELISA) kits (BD PharMingen, San Diego, CA).

Liquid chromatographyltandem mass spectrometry (LC/MS-MS) analysis. Simultaneous quantification of PGs and TXB_2 were performed as previously described [12]. Briefly, the cultured medium collected at 1 h after the stimulations were subjected to analysis by LC/MS-MS. $PGF_{2\alpha\text{-}d4}$, $PGE_{2\text{-}d4}$, $PGD_{2\text{-}d4}$, 6-keto-$PGF_{1\alpha\text{-}d4}$, and $TXB_{2\text{-}d4}$ (each 2 ng) were added into the cultured medium (0.2 ml) as an internal standard. The sample was acidified and passed through an Empore C18 HD disk cartridge (3 M Industry, St. Paul, MN). The bound fraction was collected in hexane-ethylacetate (1:2, v/v, 1 ml) as a PG-enriched fraction. After evaporating solvent, the residue was reconstituted in mobile phase (30 μl), sonicated for 30 s, and filtered. The reconstituted sample was transferred to an autosampler vial; 10 μl was subjected to the LC/MS-MS analysis. For the HPLC part, chromatography was performed on a C18 Capcell Pak MGII (1.5 × 150 mm, 5 μm) (Shiseido, Tokyo, Japan) using isocratic elution with acetonitrile–water–acetic acid (40:60:0.02 v/v) at a flow rate of 100 μl/min at 40 °C. The selected reaction monitoring was performed as previously described conditions [12].

Reverse transcriptase-polymerase chain reaction (RT-PCR). Total RNA was purified from kidney, brain, and BMMCs by using a TRIzol™ reagent (Invitrogen, Carlsbad, CA). The complementary DNA (cDNA) was prepared from 1 μg of total RNA with random hexamers and reverse transcriptase SuperScript III™ (Invitrogen). Polymerase chain reaction (PCR) was performed with following primers: 5′-GCTCTTGGTGT TTCCTTCTCG-3′ and 5′-TGCTTGCTGGCTCTCCTTCTC-3′ for a mouse F prostanoid receptor (FP) (446 bp), and 5′-CAGGAGATGG CCACTGCCGCA-3′ and 5′-CTCCTTCTGCATCCTGTCAGCA-3′ for mouse β-actin (276 bp). The annealing temperature in the PCR was set at 60 °C for FP and 52 °C for β-actin.

Statistical analysis. Difference between two mean values was evaluated by two-tail *t*-test or, in case of multiple comparison, the *t*-test combined with Bonferroni correction following ANOVA. P value less than 0.05 was regarded as statistically significant.

Results and discussion

Autocrine PGs influence cytokine production on TLR4-mediated BMMC activation

To estimate the role of autocrine PGs and LTs in LPS-dependent BMMC activation, the inhibitory effect of the Cox or 5-Lox inhibitor was measured by examining the effect on cytokine production. The Cox and Lox inhibitors significantly suppressed IL-6 production (Fig. 1A). The Cox-selective inhibitors NS398 and SC560 did not significantly inhibit TNF-α production; however, the other inhibitors significantly suppressed TNF-α production (Fig. 1B). These findings indicate the role of autocrine PGs and LTs in enhancing cytokine production following TLR4-mediated BMMC activation.

BMMCs constitutively produce $PGF_{2\alpha}$, TXB_2, and 6-keto-$PGF_{1\alpha}$

To identify the autocrine PGs from BMMCs, we simultaneously measured the cumulative amounts of $PGF_{2\alpha}$, PGE_2, PGD_2, 6-keto-$PGF_{1\alpha}$ as PGI_2 metabolites and PGJ_2 and TXB_2 as TXA2 metabolites in the BMMC culture medium by LC/MS-MS, as described previously [12]. The following three culture conditions were tested: untreated, treated with LPS (100 ng/ml), and treated with IgE/Ag (1 ng/ml TNP-OVA). A significant amount of $PGF_{2\alpha}$, TXB_2, and 6-keto-$PGF_{1\alpha}$ was detected under all the conditions (Table 1). $PGF_{2\alpha}$ and 6-keto-$PGF_{1\alpha}$ were undetectable in the culture medium, and an increase of TXB_2 was detected in the presence of BMMC, indicating that $PGF_{2\alpha}$, TXB_2, and 6-keto-$PGF_{1\alpha}$ are constitutively released from BMMCs. The stimulation with IgE/Ag but

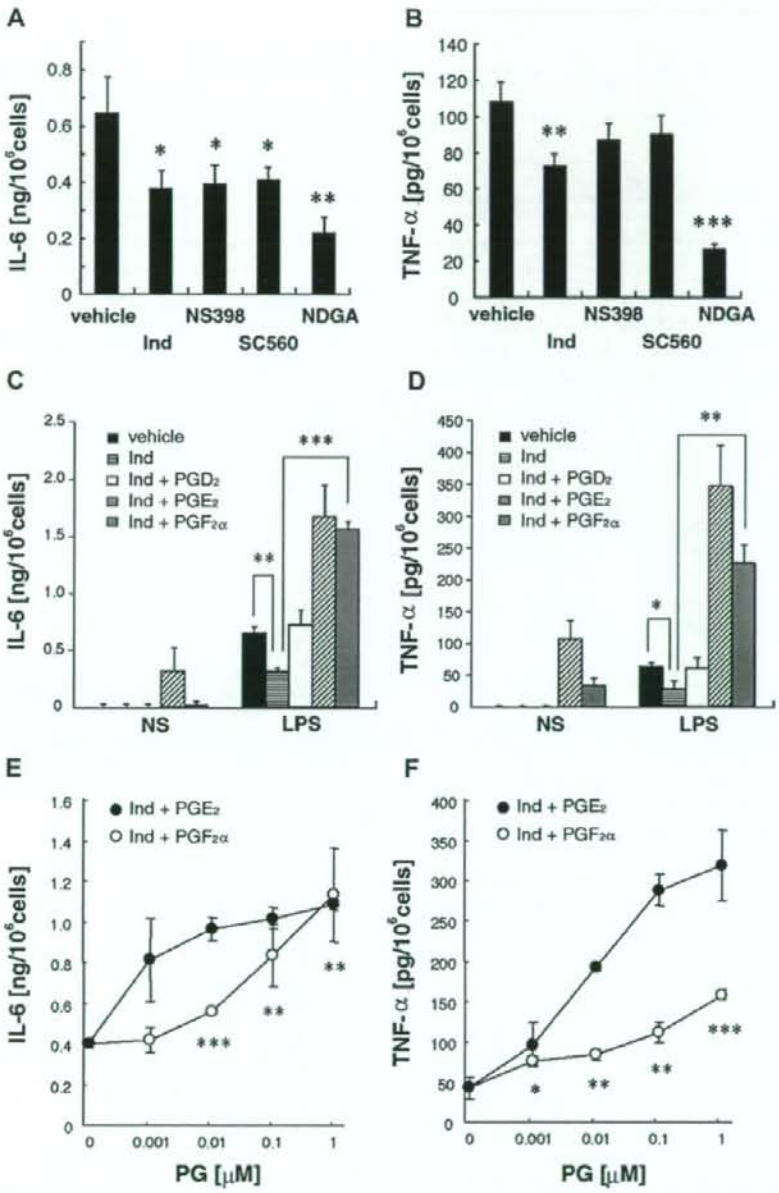

Fig. 1. Effect of deprivation and supplementation of PGs on LPS-induced cytokine responses of BMMCs. (A and B) Effect of Cox or Lox inhibition on LPS-induced cytokine response. BMMCs were cultured for 30 min with 10 μM indomethacin (Ind), 10 μM NS-398 (NS398), 20 nM SC560 (SC560), 10 μM NDGA (NDGA), or ethanol (vehicle), and then stimulated for 6 h with LPS (0.1 μg/ml). (C and D) Effect of supplemented PG on untreated or LPS-induced cytokine response. BMMCs were incubated for 30 min with 10 μM indomethacin (Ind) or DMSO (vehicle), further incubated for 20 min with 1 μM of PGD_2, PGE_2, $PGF_{2\alpha}$, or ethanol, then stimulated for 6 h with LPS (0.1 μg/ml). (E and F) The relationship between a PG dose and cytokine response of BMMCs. BMMCs were treated with PGs (0.001–1 μM). A bar represents SD of triplicate samples. Significant differences are shown: $^{*}p < 0.05$; $^{**}p < 0.01$; $^{***}p < 0.001$. The significant differences were confirmed by two experiments.

not LPS increased the release of $PGF_{2\alpha}$ and TXB_2 by 340% and 200%, respectively, of the resting level. Prior to the present study, Schleimer et al. first measured $PGF_{2\alpha}$ in the culture medium of human lung mast cells by radioimmunoassay and estimated the concentration under the untreated and IgE/Ag-induced conditions as 0.3 ng/10^6

Table 1
Quantification of BMMC-derived prostanoids and thromboxane in cultured medium[a]

	PGD_2 (pg/10^6 cells)	PGE_2 (pg/10^6 cells)	$PGF_{2\alpha}$ (pg/10^6 cells)	PGJ_2 (pg/10^6 cells)	TXB_2 (pg/10^6 cells)	6-Keto $PGF_{1\alpha}$ (pg/10^6 cells)
Medium	<10	<10	<10	<10	166 (45.5)	<10
Untreated	<10	<10	84.2 (50.2)	<10	791 (128)	253 (25.6)
LPS	<10	<10	60.0 (15.9)	<10	701 (121)	98.6 (35.6)
IgE/Ag	890 (236)	<10	288 (47.9)	<10	1593 (320)	88.6 (26.0)

[a] Values denote a mean (SD) of eicosanoid concentration of six independent samples prepared from an experiment. BMMCs were stimulated without (untreated) or with 0.1 μg/ml LPS (LPS), or 1 ng/ml TNP-OVA following IgE sensitization (IgE/Ag). Culture supernatants were collected at 1 h after stimulation. PG, prostaglandin; TX, thromboxane.

cells and 3.3 ng/10^6 cells, respectively [13]. These amounts of $PGF_{2\alpha}$ are mostly comparable to our results. PGD_2 was detected on IgE/Ag stimulation, as previously reported [14–16]. PGE_2 and PGJ_2 were undetectable under all the conditions.

$PGF_{2\alpha}$ enhances TLR4-mediated mast cell responses

Each effect of supplementation with $PGF_{2\alpha}$ and PGE_2 on the cytokine response of BMMCs was evaluated under a condition in which the production of endogenous PGs was prevented by blocking their *de novo* syntheses with indomethacin. $PGF_{2\alpha}$ as well as PGE_2 remarkably enhanced LPS-induced IL-6 (Fig. 1C) and TNF-α production (Fig. 1D). In the absence of stimulation, PGE_2-induced the production of both IL-6 and TNF-α; however, $PGF_{2\alpha}$-induced TNF-α to a lesser extent than PGE_2. PGD_2 had little effect on the cytokine production of BMMCs. The enhancement of the LPS-dependent responses by $PGF_{2\alpha}$ was observed in a dose-dependent manner (Fig. 1E and F). However, the dose–effect relationship demonstrated that $PGF_{2\alpha}$ was less effective in enhancing the LPS-dependent responses than PGE_2.

With regard to the observed effect of $PGF_{2\alpha}$, three possible mechanisms remained to be clarified at this time: the direct effect of $PGF_{2\alpha}$, the effect of conversion of the $PGF_{2\alpha}$ to PGE_2, and the effect of the contamination of PGE_2. The conversion of $PGF_{2\alpha}$ to PGE2 occurs by the action of 9-keto reductase. This enzymatic activity in untreated and stimulated BMMCs was roughly estimated by measuring the *de novo* PGE_2 synthesis in the culture incubated with $PGF_{2\alpha}$ and an excess of the BMMC lysate. There was no detectable PGE2 after the incubation (data not shown). We also estimated the level of contamination of the $PGF_{2\alpha}$ used in this study with PGE_2. The results showed that the contamination level was no higher than 0.01% of the amount of $PGF_{2\alpha}$ input (data not shown). If PGE_2 contamination was maximum in the $PGF_{2\alpha}$-supplemented culture, its effect could not have reached the level achieved by the same amount of purified PGE_2 (Fig. 1E and F). The overall findings suggest that the direct effect of $PGF_{2\alpha}$ is responsible for the enhancement of TLR-mediated mast cell responses.

There is a growing interest in understanding novel $PGF_{2\alpha}$ functions. $PGF_{2\alpha}$ has been shown to exert pleiotropic effects in a variety of pathophysiological conditions through a selective prostanoid receptor for $PGF_{2\alpha}$ (FP). The activation of FP results in an increase in the cytosolic ionic calcium and cyclic AMP concentrations and leads to the contraction of muscle fibers in smooth muscle cells [17,18]. Therefore, FP agonists, such as fluprostenol, have been used in the treatment of patients with glaucoma and for inducing labor. Recently, topical application of an FP agonist on mouse dorsal skin has been shown to stimulate hair growth [19]. FP has been shown to be expressed in the

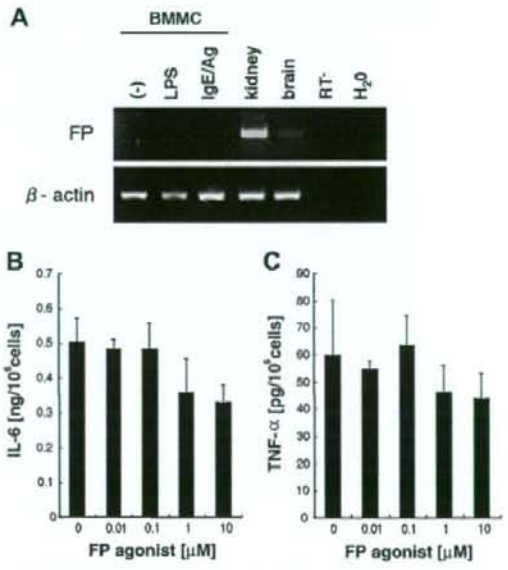

Fig. 2. Expression and function of an F prostanoid receptor (FP) in BMMCs. (A) Undetectable expression of FP in BMMCs revealed by RT-PCR with FP specific primers. Total RNA was isolated from BMMC untreated (−), LPS-induced (LPS), and IgE/Ag-induced (IgE/Ag) BMMCs, and kidney (kidney), and whole brain (brain). BMMCs were treated for 2 h with LPS (0.1 μg/ml) or TNP-specific IgE (1 μg/ml) and TNP-OVA (1 ng/ml). PCR products were visualized by ethidium bromide staining on 2% agarose gel. Amplification of β-actin shows the presence of complementary DNA in RT-PCR. A sample without RT reaction (RT^-) and water (H_2O) were used as negative references. (B and C) Unresponsiveness of BMMCs to an FP-selective agonist—fluporstenol. BMMCs were treated with LPS in the presence of indomethacin and, in place of a PG, 1 μM fluprostenol as performed in this figure. A bar represents SD of triplicate samples. Similar findings that was without statistical significance were obtained from two independent experiments.

collecting duct of the kidneys and regulate water absorption [20]. On the other hand, the presence of TXB_2 and 6-keto-$PGF_{1\alpha}$ in the cultured medium of BMMCs indicates spontaneous production of TXA_2 and PGI_2 from BMMCs. Previous studies have provided evidences for the production of TXB_2 and 6-keto-$PGF_{1\alpha}$ in human lung mast cells and rat serosal mast cells, respectively [13,21]. Other studies have shown that BMMCs respond to PGI_2 [11], and that mastocytoma P815 cells express a selective prostanoid receptor to PGI_2 [22]. The expression of the TXA_2 receptor has not been shown in mast cells [23]. Our present findings provide a novel insight that autocrine PGs regulate mast cell functions and, as a pathologic consequence, influence allergic manifestations in humans.

A selective prostanoid receptor for $PGF_{2\alpha}$ is neither expressed nor functioning in BMMCs

Our findings suggested the presence of a functional receptor for $PGF_{2\alpha}$ in BMMCs. Since the expression of FP in BMMCs had not been observed yet, we examined the expression of FP by reverse transcriptase-polymerase chain reaction (RT-PCR) by using an FP-selective agonist, namely, fluprostenol. The RT-PCR failed to show the expression of FP in untreated and stimulated BMMCs (Fig. 2A). Further, fluprostenol was shown to have no effect on the TLR4-mediated cytokine response of BMMCs (Fig. 2B). These findings suggest the absence of FP in BMMCs and favor a possibility that prostanoid receptor(s)

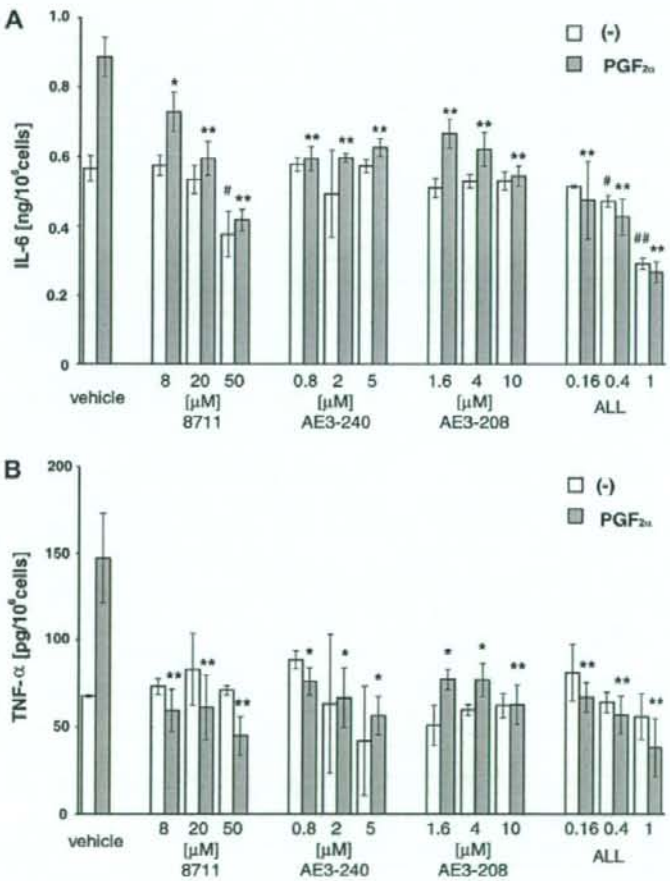

Fig. 3. Blocking effect of EP antagonist(s) on LPS-induced cytokine responses. BMMCs were incubated for 30 min with EP1 antagonist (ONO-8711, 8711), EP3 antagonist (ONO-AE3-240, AE3-240), EP4 antagonist (ONO-AE3-208, AE3-208), a mixture of three EP antagonists (ALL), or DMSO (vehicle), and then incubated for another 20 min with ethanol (white column) or 1 μM $PGF_{2\alpha}$ (gray column). The pretreated BMMCs were stimulated for 6 h with 0.1 μg/ml LPS. DMSO concentration was uniformed at 0.1% for the single antagonist use or 0.25% for the mixture use of three antagonists. For the mixture use, a mixture of 50 μM ONO-8711, 5 μM ONO-AE3-240, and 10 μM ONO-AE3-208 was arbitrarily defined as 1 U in this study. A bar represents SD of triplicate samples. Significant differences are shown: $^{*}p < 0.05$; $^{**}p < 0.01$ (vs vehicle with $PGF_{2\alpha}$); $^{\#}p < 0.05$; $^{\#\#}p < 0.01$ (vs vehicle with (−)).The significant differences were confirmed by other two experiments.

other than FP is (are) present in BMMCs to mediate the $PGF_{2\alpha}$-dependent effect.

Prostanoid receptors for PGE_2 mediate $PGF_{2\alpha}$ signals in BMMCs

Previous studies have shown that $PGF_{2\alpha}$ binds to EP1 and EP3 *in vitro*, although this heterologous association occurs with an affinity that is lower than that between PGE_2 and these receptors [24,25]. Since BMMCs have been shown to express all the four EPs, i.e., EP1, EP2, EP3, and EP4 [11], it is possible that EPs mediated the $PGF_{2\alpha}$ signals in the present experimental conditions. To test this possibility, we performed experiments using EP-selective antagonists—ONO-8711, ONO-AE3-240, and ONO-AE3-208—which have been shown to inhibit the signal of EP1, EP3, and EP4, respectively [26,27]. Two conditions with or without $PGF_{2\alpha}$ were adopted in these experiments. As a result, the augmented fraction, which is shown as the difference between the neighboring white and gray columns in Fig. 3, was significantly decreased by each of the EP antagonists as well as a mixture of all three of them. The decrease in the IL-6 response by EP1 and EP4 and in the TNF-α response by EP4 was observed in a dose-dependent manner. These findings indicate that EP1, EP3, and EP4 are potent receptors for mediating $PGF_{2\alpha}$ signals in BMMCs. Moreover, it should be noted that in the culture condition without $PGF_{2\alpha}$ supplementation, either the EP1 antagonist or the mixture containing all three antagonists significantly inhibited the IL-6 response. This finding implicates the role of endogenous $PGF_{2\alpha}$ in the cytokine response of BMMCs though EPs.

This is the first study that has identified the allergenic *in vitro* effect of $PGF_{2\alpha}$ on mast cell activation and the functional interaction between $PGF_{2\alpha}$ and EPs in mast cells. In other studies, a higher level of $PGF_{2\alpha}$ was detected in the bronchoalveolar lavages of asthmatic patients, although the cells producing $PGF_{2\alpha}$ were unidentified in these cases [28,29]. These findings encourage further investigation of whether the mechanism proposed by us is implicated in the pathogenesis of allergic diseases in humans.

References

[1] H. Qiao, M.V. Andrade, F.A. Lisboa, K. Morgan, M.A. Beaven, FcεR1 and toll-like receptors mediate synergistic signals to markedly augment production of inflammatory cytokines in murine mast cells, Blood 107 (2006) 610–618.

[2] Y.I. Nigo, M. Yamashita, K. Hirahara, R. Shinnakasu, M. Inami, M. Kimura, A. Hasegawa, Y. Kohno, T. Nakayama, Regulation of allergic airway inflammation through toll-like receptor 4-mediated modification of mast cell function, Proc. Natl. Acad. Sci. USA 103 (2006) 2286–2291.

[3] C. Braun-Fahrlander, J. Riedler, U. Herz, W. Eder, M. Waser, L. Grize, S. Maisch, D. Carr, F. Gerlach, A. Bufe, R.P. Lauener, R. Schierl, H. Renz, D. Nowak, E. von Mutius, The Allergy and Endotoxin Study Team, Environmental exposure to endotoxin and its relation to asthma in school-age children, N. Engl. J. Med. 34 (2002) 869–877.

[4] R. Friedman, M. Ackerman, E. Wald, M. Casselbrant, G. Friday, P. Fireman, Asthma and bacterial sinusitis in children, J. Allergy. Clin. Immunol. 74 (1984) 185–189.

[5] B.S. Baker, The role of microorganisms in atopic dermatitis, Clin. Exp. Immunol. 144 (2006) 1–9.

[6] S.G. Trivedi, J. Newson, R. Rajakariar, T.S. Jacques, R. Hannon, Y. Kanaoka, N. Eguchi, P. Colville-Nash, D.W. Gilroy, Essential role for hematopoietic prostaglandin D2 synthase in the control of delayed type hypersensitivity, Proc. Natl. Acad. Sci. USA 103 (2006) 5179–5184.

[7] K. Kabashima, D. Sakata, M. Nagamachi, Y. Miyachi, K. Inaba, S. Narumiya, Prostaglandin E2-EP4 signaling initiates skin immune responses by promoting migration and maturation of Langerhans cells, Nat. Med. 9 (2003) 744–749.

[8] N. Miyahara, K. Takeda, S. Miyahara, C. Taube, A. Joetham, T. Koya, S. Matsubara, A. Dakhama, A.M. Tager, A.D. Luster, E.W. Gelfand, Leukotriene B4 receptor-1 is essential for allergen-mediated recruitment of CD8+ T cells and airway hyperresponsiveness, J. Immunol. 174 (2005) 4979–4984.

[9] I. Leal-Berumen, P. O'Byrne, A. Gupta, C. Richards, J. Marshall, Prostanoid enhancement of interleukin-6 production by rat peritoneal mast cells, J. Immunol. 154 (1995) 4759–4767.

[10] C. Feng, E.M. Beller, S. Bagga, J.A. Boyce, Human mast cells express multiple EP receptors for prostaglandin E2 that differentially modulate activation responses, Blood 107 (2006) 3243–3250.

[11] M. Nguyen, M. Solle, L.P. Audoly, S.L. Tilley, J.L. Stock, J.D. McNeish, T.M. Coffman, D. Dombrowicz, B.H. Koller, Receptors and signaling mechanisms required for prostaglandin E2-mediated regulation of mast cell degranulation and IL-6 production, J. Immunol. 169 (2002) 4586–4593.

[12] T. Hishinuma, K. Suzuki, M. Saito, Y. Hamaguchi, N. Suzuki, Y. Tomioka, I. Kaneko, M. Ono, J. Goto, Simultaneous quantification of seven prostanoids using liquid chromatography/tandem mass spectrometry: the effects of arachidonic acid on prostanoid production in mouse bone marrow-derived mast cells, Prostaglandins Leukot. Essent. Fatty Acids 76 (2007) 321–329.

[13] R.P. Schleimer, E.S. Schulman, D.W. MacGlashan Jr., S.P. Peters, E.C. Hayes, G.K. Adams 3rd., L.M. Lichtenstein, N.F. Adkinson Jr., Effects of dexamethasone on mediator release from human lung fragments and purified human lung mast cells, J. Clin. Invest. 71 (1983) 1830–1835.

[14] F. Levi-Schaffer, E. Dayton, K. Austen, A. Hein, J. Caulfield, P. Gravallese, F. Liu, R. Stevens, Mouse bone marrow-derived mast cells cocultured with fibroblasts. Morphology and stimulation-induced release of histamine, leukotriene B4, leukotriene C4, and prostaglandin D2, J. Immunol. 139 (1987) 3431–3441.

[15] C. Pitton, L. Michel, P. Salem, M. Benhamou, J. Mencia-Huerta, J. Maclouf, C. Prost, C. Burtin, L. Dubertret, J. Benveniste, Biochemical and morphological modifications in dexamethasone-treated mouse bone marrow-derived mast cells, J. Immunol. 141 (1988) 2437–2444.

[16] J. Robin, D. Seldin, K. Austen, R. Lewis, Regulation of mediator release from mouse bone marrow-derived mast cells by glucocorticoids, J. Immunol. 135 (1985) 2719–2726.

[17] W. Chen, T. Andom, P. Bhattacherjee, C. Paterson, Intracellular calcium mobilization following prostaglandin receptor activation in human ciliary muscle cells, Curr. Eye. Res. 16 (1997) 847–853.

[18] B.W. Griffin, P.E. Magnino, I.-H. Pang, N.A. Sharif, Pharmacological characterization of an FP prostaglandin receptor on rat vascular smooth muscle cells (A7r5) Coupled to phosphoinositide turnover and intracellular calcium mobilization, J. Pharmacol. Exp. Ther. 286 (1998) 411–418.

[19] S. Sasaki, Y. Hozumi, S. Kondo, Influence of prostaglandin F2 and its analogues on hair regrowth and follicular melanogenesis in a murine model, Exp. Dermatol. 14 (2005) 323–328.

[20] R.L. Hebert, M. Carmosino, O. Saito, G. Yang, C.A. Jackson, Z. Qi, R.M. Breyer, C. Natarajan, A.N. Hata, Y. Zhang, Y. Guan, M.D. Breyer, Characterization of a rabbit kidney prostaglandin $F_{2\alpha}$

receptor exhibiting G(i)-restricted signaling that inhibits water absorption in the collecting duct, J. Biol. Chem. 280 (2005) 35028–35037.
[21] R.A. Lewis, N.A. Soter, P.T. Diamond, K.F. Austen, J.A. Oates, L.J. Roberts 2nd., Prostaglandin D2 generation after activation of rat and human mast cells with anti-IgE, J. Immunol. 129 (1982) 1627–1631.
[22] N. Hatae, A. Kita, S. Tanaka, Y. Sugimoto, A. Ichikawa, Induction of adherent activity in mastocytoma P-815 cells by the cooperation of two prostaglandin E2 receptor subtypes, EP3 and EP4, J. Biol. Chem. 278 (2003) 17977–17981.
[23] K.A. Knauer, J.E. Fish, N.F. Adkinson Jr., L.M. Lichtenstein, S.P. Peters, H.H. Newball, Platelet activation in antigen-induced bronchoconstriction, N. Engl. J. Med. 305 (1981) 892–893.
[24] A. Watabe, Y. Sugimoto, A. Honda, A. Irie, T. Namba, M. Negishi, S. Ito, S. Narumiya, A. Ichikawa, Cloning and expression of cDNA for a mouse EP1 subtype of prostaglandin E receptor, J. Biol. Chem. 268 (1993) 20175–20178.
[25] Y. Sugimoto, T. Namba, A. Honda, Y. Hayashi, M. Negishi, A. Ichikawa, S. Narumiya, Cloning and expression of a cDNA for mouse prostaglandin E receptor EP3 subtype, J. Biol. Chem. 267 (1992) 6463–6466.
[26] K. Watanabe, T. Kawamori, S. Nakatsugi, T. Ohta, S. Ohuchida, H. Yamamoto, T. Maruyama, K. Kondo, F. Ushikubi, S. Narumiya, T. Sugimura, K. Wakabayashi, Role of the prostaglandin E receptor subtype EP1 in colon carcinogenesis, Cancer Res. 15 (1999) 5093–5096.
[27] I. Takasaki, H. Nojima, K. Shiraki, Y. Sugimoto, A. Ichikawa, F. Ushikubi, S. Narumiya, Y. Kuraishi, Involvement of cyclooxygenase-2 and EP3 prostaglandin receptor in acute herpetic but not postherpetic pain in mice, Neuropharmacology 49 (2005) 283–292.
[28] M.C. Liu, E.R. Bleecker, L.M. Lichtenstein, A. Kagey-Sobotka, Y. Niv, T.L. McLemore, S. Permutt, D. Proud, W.C. Hubbard, Evidence for elevated levels of histamine, prostaglandin D2, and other bronchoconstricting prostaglandins in the airways of subjects with mild asthma, Am. Rev. Respir. Dis. 142 (1990) 126–132.
[29] A. Szczeklik, S. Kladek, R. Dworski, E. Nizankowska, J. Soja, J. Sheller, J. Oates, Bronchial aspirin challenge causes specific eicosanoid response in aspirin-sensitive asthmatics, Am. J. Respir. Crit. Care Med. 154 (1996) 1608–1614.

FEBS Letters 582 (2008) 2431–2434

Crucial role of peroxiredoxin III in placental antioxidant defense of mice

Lianqin Li[a,b,*], Wataru Shoji[a], Hiroaki Oshima[a], Masuo Obinata[a], Manabu Fukumoto[c], Naoko Kanno[c]

[a] Department of Cell Biology, Institute of Development, Aging, and Cancer, Tohoku University, Sendai 980-8575, Japan
[b] Department of Obstetrics and Gynecology, Peking University First Hospital, 1 Xi'anmen Dajie, Xicheng District, Beijing 100034, China
[c] Department of Pathology, Institute of Development, Aging, and Cancer, Tohoku University, Sendai 980-8575, Japan

Received 28 May 2008; accepted 30 May 2008

Available online 9 June 2008

Edited by Barry Halliwell

Abstract **We observed frequent stillbirth in peroxiredoxin III (PrxIII) knockout maternal mice. Quantitative real time PCR (qRT-PCR) and Western-blot analysis revealed increased oxidative stress in placentas that were deficient in PrxIII. We did not find significant difference between PrxIII knockout maternal mice and wild-type littermates in hematological parameters, fetal number, and embryonic development. Nevertheless, we noticed enhanced expression of PrxI in erythrocytes of pregnant knockout mice. Our results provided in vivo evidence that PrxIII played a crucial role in placental antioxidant defense. Up-regulation of PrxI might provide a compensation that protected erythrocytes against oxidative damage.**

Keywords: Stillbirth; Peroxiredoxin III (PrxIII); Placenta; Oxidative stress

1. Introduction

As a member of peroxiredoxin (Prx) family, PrxIII was predominantly localized in mitochondria and was considered to play an important role in mitochondrial antioxidant defense [1–3]. Mammalian PrxIII has two active cysteines that reduce H_2O_2 with the use of electrons provided by thioredoxin [4]. Recently, we studied in vivo function of PrxIII using PrxIII knockout (PrxIII−/−) mice. Severe lung inflammation and oxidized DNA/protein in alveolar epithelium were detected in PrxIII−/− mice exposed to intratracheal inoculation of lipopolysaccharide (LPS), indicating that PrxIII was an indispensable scavenger of reactive oxygen species (ROS) in mouse lungs under oxidative stress [5].

During the preparation of experimental mice, we observed frequent stillbirth in PrxIII−/− maternal mice. Since PrxIII was previously suggested to play an important role in placenta under oxidative stress [6,7], we were interested in analyzing in vivo function of PrxIII in pregnancy. According to previous studies, oxidative stress was relatively high in pregnancy and was further increased during labor [8,9]. On the other hand, antioxidant activity was accordingly increased with gestational progression to protect against oxidative damage [10,11]. Abundance of ROS or decrease of antioxidant activity would disturb oxidative balance and ultimately result in pathological changes. For example, a pregnant complication in human beings called pre-eclampsia was related to oxidative stress [12].

In the present study, we compared pregnant outcomes between PrxIII−/− maternal mice and wild-type (PrxIII+/+) littermates. We also investigated hematological parameters, fetal number, embryonic development, and placental oxidative stress in maternal mice.

2. Materials and methods

2.1. Mouse mating

PrxIII−/− mice were generated as described before [5]. We mated C57BL/6 (B6) mice with PrxIII−/− mice to generate PrxIII+/− offspring. The offspring were then intercrossed to produce PrxIII+/+, PrxIII+/−, and PrxIII−/− littermates for experiments.

2.2. Hematological examination on peripheral blood and histological inspection on placentas

Peripheral blood was examined on mice before pregnancy and at the 18th day of pregnancy. Hematological parameters included erythrocyte count, reticulocyte count, and hematocrit. In addition, existence of Heinz body in erythrocytes was examined on smears stained with brilliant cresyl blue.

Placentas were removed from maternal mice that were pregnant for 18 days. Two pathologists without knowledge of PrxIII genotypes examined placental sections after HE-staining.

2.3. Analysis of oxidative state in placentas

Eighteen-day placentas were homogenized and protein concentration was detected by Bio-Rad protein assay kit. After separation on 15% SDS–PAGE and transfer to Immobilon membrane (Millipore Corporation), lipid oxidation was estimated with anti-4-hydroxy-2-nonenal (4-HNE) monoclonal antibody (Japan Institute for Control of Aging, Fukuroi, Japan). Visualization was achieved with ECL Western-blotting detection system (Amersham). Anti-β-actin antibody (Sigma) was used as internal control.

In a separate experiment, RNA samples were prepared from placentas. After synthesis of first-strand cDNA, quantitative real time PCR (qRT-PCR) was performed to analyze expressions of prepro-endothelin 1 (prepro-ET-1) and tumor necrosis factor alpha (TNF-α). Primer sequences are indicated in Table 1. β-Actin was used as internal control. SYBR® GreenER™ Two-step qRT-PCR Kits was purchased from Invitrogen. qRT-PCR was performed on Bio-Rad iCycler by the following program: 95 °C 3 min, (95 °C 15 s, 60 °C

*Corresponding author. Address: Department of Obstetrics and Gynecology, Peking University First Hospital, 1 Xi'anmen Dajie, Xicheng District, Beijing 100034, China. Fax: +86 10 88257362.
E-mail address: lilq2005@126.com (L. Li).

Abbreviations: Prx, peroxiredoxin; qRT-PCR, quantitative real time polymerase chain reaction; LPS, lipopolysaccharide; ROS, reactive oxygen species; 4-HNE, 4-hydroxy-2-nonenal; Prepro-ET-1, prepro-endothelin 1; TNF-α, tumor necrosis factor alpha; PBS, phosphate-buffered saline

0014-5793/$34.00
doi:10.1016/j.febslet.2008.05.050

Table 1
Primer sequences for qRT-PCR analysis

Genes	Forward	Reverse
prepro-ET-1	5′-CTGGACATCATCTGGGTCAA-3′	5′-CTGCTTGGCAGAAATTCCA-3′
TNF-α	5′-GATTATGGCTCAGGGTCCAA-3′	5′-CCCATTTGAGTCCTTGATGG-3′
PrxI	5′-CTGCCAAGTGATTGGTGCTT-3′	5′-CCCATAATCCTGAGCAATGGT-3′
PrxII	5′-AGATCATCGCGTTCAGCAAC-3′	5′-CAAGCGTCTGGTCACGTCAG-3′
PrxIII	5′-CAGCCGTTGTCAATGGAGAG-3′	5′-TCACATCGTGAAATTCGTTAGC-3′
β-Actin	5′-ACGTTGACATCCGAAAGACC-3′	5′-CCACCGATCCACACAGAGTA-3′

60 s) × 40. Reaction volume was 50 μl. Expression of oxidative makers was calculated by equation $2^{-\Delta Ct} \times 10^6$, where $\Delta Ct = [Ct_{prepro\text{-}ET\text{-}1}$ (or $Ct_{TNF\text{-}\alpha}) - Ct_{\beta\text{-}actin}]$. Three separate reactions were performed for each gene.

2.4. Analysis of PrxI, PrxII, and PrxIII expression in erythrocytes

Total blood (about 1 ml) was obtained from mice that were pregnant for 18 days. Red blood cells were isolated with Ficoll-Paque (Pharmacia Biotech) and washed two times with phosphate-buffered saline (PBS). RNA and cell lysates were, respectively, prepared from isolated erythrocytes. Expression of PrxI, PrxII, and PrxIII was detected by qRT-PCR and Western blot. Primer sequences for qRT-PCR are indicated in Table 1. For Western-blot analysis, we used rabbit anti-PrxIII serum immunized with PrxIII C-terminal oligopeptide [5].

2.5. Statistic analysis

For qRT-PCR results, relative expression of detected genes was compared among PrxIII+/+, PrxIII+/−, and PrxIII−/− samples by analysis of variance. $P < 0.05$ was considered to be statistically significant.

3. Results

3.1. Breeding abnormality in PrxIII−/− maternal mice

After successful generation of PrxIII−/− mice, we mated PrxIII−/− mice with wild-type (B6) ones to produce heterozygous offspring (PrxIII+/−), which were intended to intercross to generate PrxIII+/+, PrxIII+/−, and PrxIII−/− littermates for experiment. Unexpectedly, we noticed that live newborns from individual PrxIII−/− maternal mouse were only 1–3, or even zero (mean litter size: 1.2 ± 0.5, $n = 6$), while B6 maternal mice gave birth to 5–8 live newborns (mean litter size: 6.7 ± 0.5, $n = 6$).

To confirm our observation, we mated PrxIII+/+ and PrxIII−/− male mice with PrxIII+/+, PrxIII+/− and PrxIII−/− female littermates, respectively. Offspring number from PrxIII−/− maternal mice (mean litter size: 0.8 ± 0.3, $n = 6$) was much smaller than that from PrxIII+/+ (mean litter size: 7.5 ± 0.3, $n = 6$) and PrxIII+/− (mean litter size: 7.2 ± 0.2, $n = 6$) maternal littermates. Therefore, pregnant outcome was only related to genotypes of female mice. We then closely monitored maternal mice around delivery time and found that newborns were already dead at birth.

To understand fetal features before delivery, we killed pregnant mice on the 18th day of second gestation and found that fetuses in PrxIII−/− maternal mice were still alive. The mean fetal numbers were 7.3 ± 0.7 for PrxIII+/+, 7.3 ± 0.5 for PrxIII+/−, and 7.0 ± 0.8 for PrxIII−/− maternal mice, while the mean fetal weights were 1.442 ± 0.072 g ($n = 44$), 1.326 ± 0.09 g ($n = 44$), and 1.285 ± 0.065 g ($n = 42$), respectively. There was no difference in fetal number or fetal weight among maternal mice with different genotypes.

3.2. Hematological parameters and placental histology

Hematological parameters were not different among PrxIII+/+, PrxIII+/−, and PrxIII−/− mice (Table 2), and no Heinz body was observed in erythrocytes (data not shown). In detail, both erythrocyte count and hematocrit in peripheral blood were decreased after pregnancy, especially in PrxIII−/− maternal mice, although the decrease did not reach statistical significance ($P > 0.05$). Reticulocyte count was significantly increased in pregnant mice ($P < 0.05$).

As shown in Fig. 1, focal necrosis and hyaline degeneration in trophoblast giant cells (black arrows) and degeneration in vessel walls (white arrows) were observed in placentas that were derived from PrxIII−/− maternal mice.

3.3. Increased oxidative stress in placentas of PrxIII−/− maternal mice

To further understand pathological changes related to fetal death, we examined oxidative states in placentas. As an α,β-unsaturated aldehyde derived from peroxidation of ω6-unsaturated fatty acids, 4-HNE can efficiently react with sulfhydryl groups or histidine and lysine groups of proteins to form stable 4-HNE-protein compound, which is specifically recognized by anti 4-HNE antibody [13]. As shown in Fig. 2, high level of 4-HNE-modified protein was detected in placenta of Prx III−/− maternal mice as compared with PrxIII+/+ or PrxIII+/− samples. In addition, qRT-PCR analysis revealed that expressions of prepro-ET-1 and TNF-α were 6.24- and 2.66-fold higher, respectively, in PrxIII−/− placenta than in PrxIII+/+ placenta (Fig. 3). There was no significant difference in prepro-ET-1 or TNF-α expression between PrxIII+/+ and PrxIII+/− placentas.

Table 2
Hematological parameters in mice before and after pregnancy (means ± S.E.)

Genotype ($n = 6$)	Erythrocyte (10^6/μl)		Reticulocyte (%)		Hematocrit (%)	
PrxIII+/+	9.0 ± 0.4	7.8 ± 0.3	1.3 ± 0.5	5.6 ± 1.1*	50 ± 1.8	45 ± 0.7
PrxIII+/−	8.8 ± 0.2	7.5 ± 0.2	1.3 ± 0.6	5.4 ± 0.8*	50.3 ± 2.4	44.2 ± 1.6
PrxIII−/−	8.7 ± 0.2	6.5 ± 0.3	1.4 ± 0.4	4.9 ± 1.0*	49.6 ± 0.3	40.5 ± 0.4

There was no significant difference in hematological parameters among non-pregnant mice. Erythrocyte count and hematocrit became relatively low after pregnancy, especially in PrxIII−/− maternal mice. The percentage of reticulocytes was significantly increased in pregnant mice (*$P < 0.05$). Left number: before pregnancy and right number: after pregnancy.

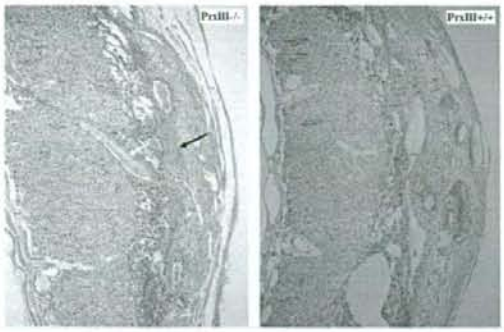

Fig. 1. Histological examination on HE-stained placental sections. Focal necrosis and hyaline degeneration in trophoblast giant cells (black arrows) and degeneration in vessel walls (white arrows) were observed in placentas derived from PrxIII−/− maternal mice. Original magnification: ×40.

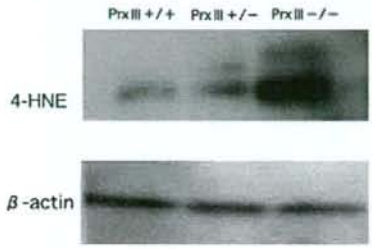

Fig. 2. Western-blot analysis for 4-HNE-modified protein in placental tissues. A signal with 51 kDa molecular size was significantly enhanced in PrxIII−/− placenta.

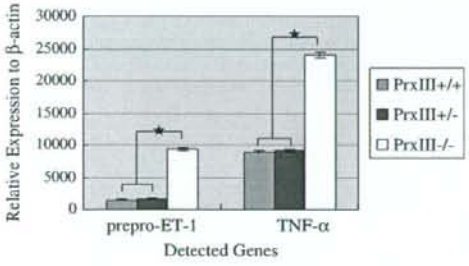

Fig. 3. Representative results of qRT-PCR for placental prepro-ET-1 and TNF-α expressions. Both prepro-ET-1 and TNF-α were significantly up-regulated in PrxIII−/− placenta as compared with PrxIII+/+ and PrxIII+/− samples (PrxIII−/− vs. PrxIII+/+ and PrxIII+/−: $^{\star}P < 0.01$).

3.4. Expression of PrxI, PrxII, and PrxIII in erythrocytes of pregnant mice

As indicated in Fig. 4, PrxIII protein was undetectable in erythrocytes of PrxIII−/− mice. However, we noticed an extra 28-kDa signal that was most enhanced in PrxIII−/− sample. Since PrxIII oligopeptide used to raise anti-PrxIII antibody shares more than 56% amino acid sequences with PrxI and PrxII C-terminals [5], the antibody might has cross-reactivity

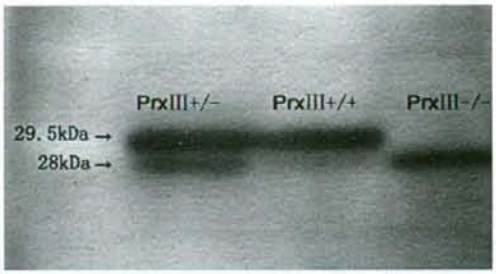

Fig. 4. Western-blot analysis for PrxIII expression in mouse erythrocytes. An extra 28 kDa signal was observed and was most enhanced in PrxIII−/− sample that was deficient in PrxIII protein.

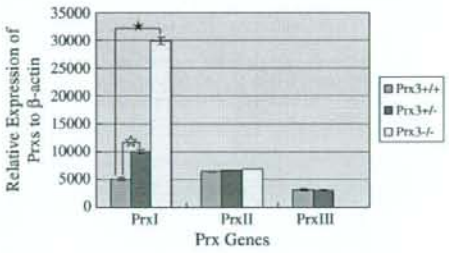

Fig. 5. Representative results of qRT-PCR for Prx expression in erythrocytes of pregnant mice. PrxI mRNA was predominantly increased in erythrocytes of PrxIII−/− and PrxIII+/− mice as compared with PrxIII+/+ littermates (PrxIII−/− vs. PrxIII+/+: $^{\star}P < 0.01$; PrxIII+/− vs. PrxIII+/+: $^{\star}P < 0.05$).

with PrxI and PrxII proteins. We supposed that the extra band represented PrxI protein as the molecular size of the signal corresponded to PrxI molecular weight. To confirm our hypothesis, we performed qRT-PCR analysis to detect mRNA of PrxI, PrxII, and PrxIII in erythrocytes of pregnant mice. The results revealed that PrxI was predominantly up-regulated by 6-fold in PrxIII−/− mice and 2-fold in PrxIII+/− mice as compared with that in PrxIII+/+ littermates (Fig. 5). We did not find significant change of Prx II expression.

4. Discussion

In the present study, we demonstrated frequent stillbirth and serious placental oxidation in PrxIII−/− maternal mice. Since fetal fates were dependent on the phenotypes of maternal mice instead of that of fetuses themselves, we suggested that mechanism of fetal death in PrxIII−/− maternal mice might be due to the functional lack of PrxIII in placenta.

In addition to placental vessel lesions, lipid oxidation was significantly increased in placentas from PrxIII−/− maternal mice. According to previous reports, oxidative stress could induce expressions of TNF-α and endothelin-1 [14–16]. Elevated level of TNF-α in PrxIII−/− mouse placentas further demonstrated increased placental oxidative stress. More importantly, high expression of placental prepro-ET-1 suggested excessive production of mature endothelin-1, which would cause vascular spasm and subsequent low blood supply in placenta. Low

blood supply, together with oxidative damage in placenta, would result in inefficient gas exchange between pregnant mice and fetuses. Under hypoxic or malperfusion conditions, ROS levels was increased in placentas [17,18], which would worsen placental oxidative stress. The situation in PrxIII−/− maternal mice reached the worst level before and during delivery and resulted in fetal hypoxia and death ultimately.

It is well known that pregnancy is accompanied with an increase of blood volume. Since plasma increases to a greater extent than erythrocyte number, the so-called "physiological anemia" occurs. Higher reticulocyte percentage in pregnant mice reflected such a state in the present study. We noticed that the situation in PrxIII−/− maternal mice was relatively serious as compared with PrxIII+/+ or PrxIII+/− littermates. Our finding added weight to recent report that PrxIII was involved in proerythrocyte differentiation [19].

Although there existed serious oxidative stress in placentas derived from PrxIII−/− maternal mice, we did not find Heinz body in erythrocytes, a marker for hemoglobin oxidation. We hypothesize that Prx I provides compensation for PrxIII deficiency on the following evidence: first, Prx I has been proved to play an important antioxidant role in erythrocytes [20]. Second, PrxIII shares more than 70% amino acid sequences with PrxI, and the two Prxs remove H_2O_2 through the same mechanism [4]. Third, the present study indicated that PrxI was significantly up-regulated in erythrocytes of pregnant PrxIII−/− mice. It might be Prx I enhancement that contributed to protection of erythrocytes against oxidative damage.

Acknowledgements: We are very grateful to Miss Kyoko Itoh for help with preparation of this manuscript.

References

[1] Watabe, S., Hiroi, T., Yamamoto, Y., Fujooka, Y., Hasegawa, H., Yago, N. and Takahashi, S.Y. (1997) SP-22 is a thioredoxin-dependent peroxide reductase in mitochondria. Eur. J. Biochem. 249, 52–60.

[2] Chae, H.Z., Kim, H.J., Kang, S.W. and Rhee, S.G. (1999) Characterization of three isoforms of mammalian peroxiredoxin that reduce peroxides in the presence of thioredoxin. Diabetes Res. Clin. Pract. 45, 101–112.

[3] Rabilloud, T., Heller, M., Rigobello, M.P., Bindoli, A., Aebersold, R. and Lunardi, J. (2001) The mitochondrial antioxidant defence system and its response to oxidative stress. Proteomics 1, 1105–1110.

[4] Rhee, S.G., Kang, S.W., Chang, T.S., Jeong, W. and Kim, K. (2001) Peroxiredoxin, a novel family of peroxidases. IUBMB Life 52, 35–41.

[5] Li, L., Shoji, W., Takano, H., Nishimura, N., Aoki, Y., Takahashi, R., Goto, S., Kaifu, T., Takai, T. and Obinata, M. (2007) Increased susceptibility of MER5 (peroxiredoxin III) knockout mice to lipopolysaccharide (LPS)-induced oxidative stress. Biochem. Biophys. Res. Commun. 355, 715–721.

[6] Ejima, K., Nanri, H., Araki, M., Koji, T., Shibata, E., Kashimura, M. and Ikeda, M. (2000) Expression of mitochondrial thioredoxin-dependent antioxidant protein, SP-22, in normal human and inflammatory mouse placentae. Placenta 21, 847–852.

[7] Shibata, E., Nanri, H., Ejima, K., Araki, M., Fukuda, J., Yoshimura, K., Toki, N., Ikeda, M. and Kashimura, M. (2003) Enhancement of mitochondrial oxidative stress and up-regulation of antioxidant protein peroxiredoxin III/SP-22 in the mitochondria of human pre-eclamptic placentae. Placenta 24, 698–705.

[8] Raijmakers, M.T., Roes, E.M., Poston, L., Steegers, E.A. and Peters, W.H. (2007) The transient increase of oxidative stress during normal pregnancy is higher and persists after delivery in women with pre-eclampsia. Eur. J. Obstet. Gynecol. Reprod. Biol., (Epub ahead of print).

[9] Cindrova-Davies, T., Yung, H.W., Johns, J., Spasic-Boskovic, O., Korolchuk, S., Jauniaux, E., Burton, G.J. and Charnock-Jones, D.S. (2007) Oxidative stress, gene expression, and protein changes induced in the human placenta during labor. Am. J. Pathol. 171, 1168–1179.

[10] Qanungo, S. and Mukherjea, M. (2000) Ontogenic profile of some antioxidants and lipid peroxidation in human placental and fetal tissues. Mol. Cell. Biochem. 215, 11–19.

[11] Carone, D., Loverro, G., Greco, P., Capuano, F. and Selvaggi, L. (1993) Lipid peroxidation products and antioxidant enzymes in red blood cells during normal and diabetic pregnancy. Eur. J. Obstet. Gynecol. Reprod. Biol. 51, 103–109.

[12] Roberts, J.M. and Lain, K.Y. (2002) Recent Insights into the pathogenesis of pre-eclampsia. Placenta 23, 359–372.

[13] Toyokuni, S., Miyake, N., Hiai, H., Hagiwara, M., Kawakishi, S., Osawa, T. and Uchida, K. (1995) The monoclonal antibody specific for the 4-hydroxy-2-nonenal histidine adduct. FEBS Lett. 359, 189–191.

[14] Hung, T.H., Charnock-Jones, D.S., Skepper, J.N. and Burton, G.J. (2004) Secretion of tumor necrosis factor-alpha from human placental tissues induced by hypoxia-reoxygenation causes endothelial cell activation in vitro: a potential mediator of the inflammatory response in preeclampsia. Am. J. Pathol. 164, 1049–1061.

[15] Ruef, J., Moser, M., Kubler, W. and Bode, C. (2001) Induction of endothelin-1 expression by oxidative stress in vascular smooth muscle cells. Cardiovasc. Pathol. 10, 311–315.

[16] Kaehler, J., Sill, B., Koester, R., Mittmann, C., Orzechowski, H.D., Muenzel, T. and Meinertz, T. (2002) Endothelin-1 mRNA and protein in vascular wall cells is increased by reactive oxygen species. Clin. Sci. Lond 103, 176S–178S.

[17] Hung, T.H., Skepper, J.N. and Burton, G.J. (2001) In vitro ischemia-reperfusion injury in term human placenta as a model for oxidative stress in pathological pregnancies. Am. J. Pathol. 159, 1031–1043.

[18] Hung, T.H. and Burton, G.J. (2006) Hypoxia and reoxygenation: a possible mechanism for placental oxidative stress in preeclampsia. Taiwan J. Obstet. Gynecol. 45, 189–200.

[19] Yang, H.Y., Jeong, D.K., Kim, S.H., Chung, K.J., Cho, E.J., Yang, U., Lee, S.R. and Lee, T.H. (2007) The role of peroxiredoxin III on late stage of proerythrocyte differentiation. Biochem. Biophys. Res. Commun. 359, 1030–1036.

[20] Neumann, C.A., Krause, D.S., Carman, C.V., Das, S., Dubey, D.P., Abraham, J.L., Bronson, R.T., Fujiwara, Y., Orkin, S.H. and Van Etten, R.A. (2003) Essential role for the peroxiredoxin Prdx1 in erythrocyte antioxidant defence and tumour suppression. Nature 424, 561–565.

British Journal of Cancer (2008) 99, 2020–2028

www.bjcancer.com

KRAS or *BRAF* mutation status is a useful predictor of sensitivity to MEK inhibition in ovarian cancer

N Nakayama[1], K Nakayama*[,1], S Yeasmin[1], M Ishibashi[1], A Katagiri[1], K Iida[1], M Fukumoto[2] and K Miyazaki[1]

[1]*Departments of Obstetrics and Gynecology, Shimane University School of Medicine, Izumo, Japan;* [2]*Departments of Pathology, Institute of Development, Aging and Cancer, Tohoku University, Sendai, Japan*

This study examined the status of *KRAS* and *BRAF* mutations, in relation to extracellular signal-regulated protein kinase (ERK) activation in 58 ovarian carcinomas to clarify the clinicopathological and prognostic significance of *KRAS/BRAF* mutations. Somatic mutations of either *KRAS* or *BRAF* were identified in 12 (20.6%) out of 58 ovarian carcinomas. The frequency of *KRAS/BRAF* mutations in conventional serous high-grade carcinomas (4.0%: 1/25) was significantly lower than that in the other histological type (32.3%: 10/31). Phosphorylated ERK1/2 (p-ERK1/2) expression was identified in 18 (38.2%) out of 45 ovarian carcinomas. *KRAS/BRAF* mutation was significantly correlated with International Federation of Gynecology and Obstetrics (FIGO) stage I, II ($P<0.001$), and p-ERK1/2 ($P<0.001$). No significant correlations between *KRAS/BRAF* mutations or p-ERK1/2 expression and overall survival were found in patients with ovarian carcinoma treated with platinum and taxane chemotherapy ($P=0.2460$, $P=0.9339$, respectively). Next, to clarify the roles of ERK1/2 activation in ovarian cancers harbouring *KRAS* or *BRAF* mutations, we inactivated ERK1/2 in ovarian cancer cells using CI-1040. CI-1040 is a compound that selectively inhibits MAP kinase kinase (MEK), an upstream regulator of ERK1/2, and thus prevents ERK1/2 activation. Profound growth inhibition and apoptosis were observed in CI-1040-treated cancer cells with mutations in either *KRAS* or *BRAF* in comparison with the ovarian cancer cells containing wild-type sequences. This was evident in both *in vitro* and *in vivo* studies. The findings in this study indicate that an activated ERK1/2 pathway is critical to tumour growth and survival of ovarian cancers with *KRAS* or *BRAF* mutations. Furthermore, they suggest that the CI-1040-induced phenotypes depend on the mutational status of *KRAS* and *BRAF* in ovarian cancers. Therefore, ovarian cancer patients with *KRAS* or *BRAF* mutations may benefit from CI-1040 treatment.

British Journal of Cancer (2008) **99,** 2020–2028. doi:10.1038/sj.bjc.6604783 www.bjcancer.com
Published online 18 November 2008

Keywords: ovarian carcinoma; *KRAS*; *BRAF*; mutation; ERK1/2; CI-1040

Translational Therapeutics

Ovarian carcinoma is the most lethal malignant disease in American women (Wingo *et al*, 1995) and the most lethal gynaecological cancer in Japan. Its frequency has increased dramatically in the last decade. In more than 70% of patients with ovarian carcinoma, there is evidence of tumour dissemination beyond the ovaries at diagnosis. In these cases, combined treatment with surgery and chemotherapy is necessary. First-line chemotherapy with platinum drugs and taxanes yields a response rate of over 80%, but almost all patients relapse. Although there are well-established surgical and chemotherapeutic treatments for ovarian cancer, there is a significant opportunity to develop drugs targeting specific molecular pathways. Drugs of this type would be particularly useful for recurrent disease that has acquired chemoresistance. Thus, there is a need for an improved understanding of the molecular pathways of ovarian carcinogenesis. Several genetic alterations are associated with ovarian carcinogenesis. The most frequent genetic abnormalities in ovarian carcinoma are mutations in *KRAS*, *BRAF*, and *p53* (Singer *et al*, 2003; Nakayama *et al*, 2006).

*Correspondence: Dr K Nakayama,Shimane University School of Medicine, Enyacho 89-1, Izumo, Shimane, Japan 6938501;
E-mail: kn88@med.shimane-u.ac.jp
Revised 10 October 2008; accepted 21 October 2008; published online 18 November 2008

Mutations of either *BRAF* or *KRAS* lead to constitutive activation (phosphorylation) of their downstream target, mitogen-activated protein kinase (MAPK), also known as extracellular signal-regulated protein kinase (ERK) (Olson and Hallahan, 2004; Wan *et al*, 2004). Mutations in *BRAF* or *KRAS* are correlated with overexpression of activated ERK1/2 in ovarian serous tumours (Hsu *et al*, 2004). Activation of ERK1/2 in turn activates downstream cellular targets (Peyssonnaux and Eychene, 2001; Allen *et al*, 2003) including a variety of cellular and nuclear proteins. Although the functions of the RAS–RAF–MEK–ERK pathway and its downstream effectors have been recently explored, only the serous type of ovarian cancer has been studied (Hsu *et al*, 2004; Pohl *et al*, 2005). In addition, the biological role of this pathway in the development of ovarian cancers of other histological types is unknown.

Activating *KRAS* and *BRAF* mutations typically show mutant exclusivity in tumours (Brose *et al*, 2002; Davies *et al*, 2002; Gorden *et al*, 2003; Singer *et al*, 2003).

A large proportion of microsatellite-stable colorectal tumour metastases has been shown to accumulate *BRAF/KRAS* mutations (Oliveira *et al*, 2007). This suggests an epistatic relationship in which either mutation is sufficient to deregulate a common effector pathway, such as the MAP kinase kinase (MEK)–ERK kinase cascade. If this is the case, tumours arising as a result of a mutation in either *KRAS* or *BRAF* should harbour similar

downstream dependencies. These might represent useful therapeutic targets in ovarian cancer. To test this hypothesis, we examined the consequences of MEK–ERK pathway inhibition using a highly potent and selective inhibitor of MEK1/2, CI-1040 (formerly known as PD184352) (Schaeffer and Weber, 1999; Sebolt-Leopold *et al*, 1999, 2003; Sebolt-Leopold, 2004). The inhibitor was tested in a collection of ovarian cancer cell lines that showed differing mechanisms of MAP kinase pathway deregulation.

MATERIALS AND METHODS

Tissue samples

Formalin-fixed, paraffin-embedded tissue samples of 58 ovarian cancers, including 27 serous carcinomas, 20 mucinous carcinomas, and 11 endometrioid carcinomas were used in this study. These samples were obtained from the Department of Obstetrics and Gynecology at the Shimane University Hospital. Diagnosis was based on conventional morphological examination of sections stained with haematoxylin and eosin (H&E) staining, and tumours were classified according to the WHO (World Health Organization) classification. Tumour staging was carried out according to the International Federation of Gynecology and Obstetrics (FIGO) classification. The clinicopathological characteristics of the patients included in this study are summarised in Table 1. All the patients were primarily treated with cytoreductive surgery and adjuvant platinum and taxane chemotherapy (CBDCA AUC5, Paclitaxel 175 mg m^{-2} or Docetaxel 70 mg m^{-2}). All the cases received 6–12 courses of this regimen. The acquisition of tumour tissues was approved by the Shimane University Institutional Review Board. The paraffin tissue blocks were organised into tissue microarrays, which were made by removing 3 mm diameter cores of tumour from each block. The areas for coring were selected by surgical pathologists (MF) on the basis of a review of the H&E slides.

Cell culture and cell lines

OVCAR3, SKOV3, A2780, MDAH2774 (serous carcinoma), and ES2 (clear cell carcinoma) human ovarian cancer cell lines were obtained from the American Tissue Culture Center (Rockville, MD, USA). The human ovarian carcinoma cell line KF28 (serous carcinoma) was a kind gift from Dr Yoshihiro Kikuchi (Ohki Memorial Kikuchi Cancer Clinic for Women, Saitama, Japan) (Yamamoto *et al*, 2000). The MPSC1 cell line was established from a low-grade serous carcinoma and was a kind gift from Dr le-Ming Shih (Johns Hopkins Medical Institutions, Baltimore, MD, USA). OVK#18 (serous carcinoma) human ovarian cancer cell line was obtained from Tohoku University (Sendai, Japan). OMC3 (mucinous carcinoma) and JHOC5 (clear cell carcinoma) human ovarian cancer cell lines were also obtained from Riken Bioresource Center (Ibaragi, Japan). In addition, human papillomavirus E6/E7-immortalised primary cultures of normal ovarian surface epithelium (OSE) were also included in this study. IOSE27, a normal OSE cell line, was obtained from the American Tissue Culture Center. OSE7 and OSE10 normal OSE cell lines were a kind gift from Dr Hidetaka Katabuchi (Kumamoto University, Kumamoto, Japan).

A set of primary cultures was established from ovarian cancers, including POC-1, POC-2, and POC-3. The acquisition of anonymous tissue specimens was approved by the Shimane University Institutional Review Board.

The diagnoses were confirmed by a surgical pathologist before the tumour samples were harvested for experiments. Primary tumour cultures were established from freshly isolated tumour samples by immunosorting or trypsinisation. For immunosorting, fresh tumour tissues were minced and incubated with collagenase

Table 1 Mutational status of *KRAS* and *BRAF* genes and p-ERK1/2 expression in ovarian cancer

Case no.	Histology	Grade	*KRAS*	*BRAF*	p-ERK1/2
1	Serous	1	WT	WT	N
2	Serous	1	WT	T1796A/V600E	P
3	Serous	2	WT	WT	N
4	Serous	3	WT	WT	N
5	Serous	3	WT	WT	N
6	Serous	2	WT	WT	P
7	Serous	2	WT	WT	N
8	Serous	2	WT	WT	P
9	Serous	3	WT	WT	N
10	Serous	3	WT	WT	P
11	Serous	3	WT	WT	P
12	Serous	3	WT	WT	N
13	Serous	3	WT	WT	N
14	Serous	3	G35T/G12V	WT	P
15	Serous	3	WT	WT	N
16	Serous	3	WT	WT	N
17	Serous	3	WT	WT	N
18	Serous	3	WT	WT	P
19	Serous	3	WT	WT	N
20	Serous	3	WT	WT	N
21	Serous	3	WT	WT	N
22	Serous	3	WT	WT	P
23	Serous	3	WT	WT	P
24	Serous	3	WT	WT	N
25	Serous	3	WT	WT	N
26	Serous	3	WT	WT	P
27	Serous	3	WT	WT	P
28	Mucinous	1	WT	T1796A/V600E	P
29	Mucinous	1	G35A/G12D	T1796A/V600E	P
30	Mucinous	1	WT	WT	N
31	Mucinous	1	WT	T1796A/V600E	P
32	Mucinous	1	G35T/G12V	WT	P
33	Mucinous	2	WT	WT	N
34	Mucinous	2	WT	WT	N
35	Mucinous	2	G35A/G12D	WT	P
36	Mucinous	2	WT	WT	N
37	Mucinous	2	WT	WT	N
38	Mucinous	2	WT	WT	N
39	Mucinous	2	WT	WT	N
40	Mucinous	2	WT	WT	P
41	Mucinous	3	WT	WT	P
42	Mucinous	3	WT	WT	N
43	Mucinous	3	WT	WT	N
44	Mucinous	3	WT	WT	N
45	Mucinous	3	WT	WT	N
46	Mucinous	3	WT	WT	P
47	Mucinous	3	WT	WT	N
48	Endometrioid	1	WT	T1796A/V600E	P
49	Endometrioid	1	WT	WT	N
50	Endometrioid	2	WT	WT	P
51	Endometrioid	2	WT	WT	N
52	Endometrioid	2	G35A/G12D	WT	P
53	Endometrioid	2	G35A/G12D	WT	P
54	Endometrioid	2	G35T/G12V	WT	P
55	Endometrioid	3	G35A/G12D	WT	P
56	Endometrioid	3	WT	WT	N
57	Endometrioid	3	WT	WT	P
58	Endometrioid	3	WT	WT	N

N = negative; P = positive; WT = wild type.